

ENERGY STABLE AND MAXIMUM BOUND PRINCIPLE PRESERVING SCHEMES FOR THE Q -TENSOR FLOW OF LIQUID CRYSTALS*

DIANMING HOU[†], XIAOLI LI[‡], ZHONGHUA QIAO[§], AND NAN ZHENG[¶]

Abstract. In this paper, we propose two efficient fully-discrete schemes for Q -tensor flow of liquid crystals by using the first- and second-order stabilized exponential scalar auxiliary variable (sESAV) approach in time and the finite difference method for spatial discretization. The modified discrete energy dissipation laws are unconditionally satisfied for both two constructed schemes. A particular feature is that, for two-dimensional (2D) and a kind of three-dimensional (3D) Q -tensor flows, the unconditional maximum-bound-principle (MBP) preservation of the constructed first-order scheme is successfully established, and the proposed second-order scheme preserves the discrete MBP property with a mild restriction on the time-step sizes. Furthermore, we rigorously derive the corresponding error estimates for the fully-discrete second-order schemes by using the built-in stability results. Finally, various numerical examples validating the theoretical results, such as the orientation of liquid crystal in 2D and 3D, are presented for the constructed schemes.

Key words. Energy stability; error estimates; maximum bound principle; Q -tensor; liquid crystal

AMS subject classifications. 65M12, 65M15, 35K35

1. Introduction. Liquid crystals are generally known as the fourth state of matter [9, 19, 20, 34], different from gases, liquids, and solids. They not only have the property of fluid flows but also possess the property of solids. For example, their molecules have a crystal-like configuration. The orientational order plays an important role in liquid crystals, which is an intermediate state of matter between solid and liquid [2, 12, 13, 15]. According to the orientational and the positional order, there are several types of liquid crystal phases, such as the nematic phase, the cholesteric phase and the smectic phase. The simplest liquid crystal phase is the nematic phase, whose rod-like molecules lack translational order but do exhibit some degree of long-range orientational order. Within the framework of the Landau–de Gennes theory [7], it is widely believed that the local orientation and order of liquid crystal molecules are characterized by a symmetric, traceless $d \times d$ tensor, which is called the Q -tensor [10, 26, 29]. We concentrate on the Q -tensor theory for nematic liquid crystal flows in this paper.

* Submitted to the editors DATE.

Funding: D. Hou is partially supported by Natural Science Foundation of China grant 12001248, NSF of Jiangsu Province grant BK20201020, Jiangsu Province Universities Science Foundation grant 20KJB110013 and Hong Kong Polytechnic University grant 1-W00D. X. Li is supported in part by the National Natural Science Foundation of China grants 12271302, 12131014. Z. Qiao is partially supported by Hong Kong Research Council RFS Grant RFS2021-5S03 and GRF Grant 15302122, Hong Kong Polytechnic University Grant 4-ZZLS, and CAS AMSS-PolyU Joint Laboratory of Applied Mathematics. N. Zheng is partially supported by the Hong Kong Polytechnic University Postdoctoral Research Fund 1-W22P.

[†]School of Mathematics and Statistics, Jiangsu Normal University, 221116 Xuzhou, China. Current address: Department of Applied Mathematics, The Hong Kong Polytechnic University, Hung Hom, Kowloon, Hong Kong. (dmhou@stu.xmu.edu.cn).

[‡]School of Mathematics, Shandong University, Jinan, Shandong, 250100, P.R. China. (xiaoli.math@sdu.edu.cn).

[§]Department of Applied Mathematics & Research Institute for Smart Energy, The Hong Kong Polytechnic University, Hung Hom, Kowloon, Hong Kong. (zqiao@polyu.edu.hk).

[¶]Corresponding author. Department of Applied Mathematics, The Hong Kong Polytechnic University, Hung Hom, Kowloon, Hong Kong. (nanzheng@polyu.edu.hk).

The Landau-de Gennes free energy functional [3, 8, 14] is given as

$$\mathcal{E}[Q] = \int_{\Omega} \mathcal{F}(Q(\mathbf{x})) d\mathbf{x},$$

where Ω is a smooth, bounded domain in \mathbb{R}^d ($d = 2, 3$) and the tensor function Q is defined in the space

$$(1.1) \quad \mathcal{S}^{(d)} \stackrel{\text{def}}{=} \left\{ M \in \mathbb{R}^{d \times d} \left| \sum_{i=1}^d M^{ii} = 0, M^{ij} = M^{ji} \in \mathbb{R}, \forall i, j = 1, \dots, d \right. \right\}.$$

Here, $\mathcal{F}(Q) = \mathcal{F}_{\text{el}} + \mathcal{F}_{\text{bulk}}$. The elastic part of the free energy density functional \mathcal{F} , denoted by \mathcal{F}_{el} , depends on the gradient of Q , while the bulk part, denoted by $\mathcal{F}_{\text{bulk}}$, depends exclusively on Q .

The bulk-free energy density $\mathcal{F}_{\text{bulk}}$ often takes the form of a truncated expansion. One can use the following simplest setting

$$(1.2) \quad \mathcal{F}_{\text{bulk}} \stackrel{\text{def}}{=} \frac{a}{2} \text{tr}(Q^2) - \frac{b}{3} \text{tr}(Q^3) + \frac{c}{4} \text{tr}^2(Q^2),$$

where the constants for the bulk material are taken to be $a \in \mathbb{R}$, $b \geq 0$ and $c > 0$. The phase, which changes from the isotropic phase to the nematic phase, is controlled by a [33]. Specifically, the system is in the isotropic phase with $a > 0$ while it is in the nematic phase with $a < 0$. It can be obtained that $b \geq 0$ in [14, 31], here $c > 0$ [21, 30] ensures that the $\mathcal{F}_{\text{bulk}}$ is bounded from below.

The strain energy density is provided by the elastic-free energy density \mathcal{F}_{el} as a result of spatial variations in the tensor order parameter. The simplest form which is invariant under rigid rotation and material symmetry is as follows

$$\mathcal{F}_{\text{el}} \stackrel{\text{def}}{=} \frac{L_1}{2} |\nabla Q|^2 + \sum_{i,j,k=1}^d \left(\frac{L_2}{2} \partial_j Q^{ik} \partial_k Q^{ij} + \frac{L_3}{2} \partial_j Q^{ij} \partial_k Q^{ik} \right),$$

where $\partial_k Q^{ij}$ represents a partial derivative of ij component of Q with respect to x_k .

The following L^2 -gradient flow in \mathbb{R}^d , $d = 2, 3$, corresponds to the energy functional $\mathcal{E}[Q]$ where Q takes values in $\mathcal{S}^{(d)}$:

$$(1.3) \quad \frac{\partial Q^{ij}}{\partial t} = - \left(\frac{\delta \mathcal{E}}{\delta Q} \right)^{ij} + \lambda \delta^{ij} + \mu^{ij} - \mu^{ji}, \quad 1 \leq i, j \leq d,$$

where the Lagrange multiplier λ corresponds to the tracelessness constraint, while $\mu = (\mu^{ij})_{d \times d}$ corresponds to the matrix symmetry constraint. The variational derivative of \mathcal{E} with respect to Q is denoted as $\delta \mathcal{E} / \delta Q$. In fact, we always impose $L_i > 0$, which ensures that the summation of the first three quadratic terms concerning L_1, L_2 and L_3 in \mathcal{F}_{el} is positive definite from a modeling perspective [30].

The evolution equation (1.3) is as follows after expansion

$$(1.4) \quad \begin{aligned} \partial_t Q^{ij} = & L_1 \Delta Q^{ij} + \frac{L_2 + L_3}{2} \left(\sum_{k=1}^d (\partial_j \partial_k Q^{ik} + \partial_i \partial_k Q^{jk}) - \frac{2}{d} \sum_{k,l=1}^d \partial_l \partial_k Q^{lk} \delta^{ij} \right) \\ & - \left(a Q^{ij} - b ((Q^2)^{ij} - \frac{1}{d} \text{tr}(Q^2) \delta^{ij}) + c \text{tr}(Q^2) Q^{ij} \right), \end{aligned}$$

for $1 \leq i, j \leq d$, with initial and boundary conditions given by

$$Q(\mathbf{x}, 0) = Q^0(\mathbf{x}), \quad \text{and} \quad Q(\mathbf{x}, t)|_{\partial\Omega} = 0.$$

There exist several numerical researches for the Q -tensor model [1, 6, 3, 8, 22, 27, 32, 33]. Cai, Shen and Xu [3] proposed a first-order nonlinear scheme for a 2D dynamic Q -tensor model of nematic liquid crystals by using a stabilizing technique, the maximum principle and convergence analysis are established. The constructed scheme in this paper can not guarantee unconditional energy stability. Gudibanda et al. [8] presented a fully discrete convergent finite difference scheme for the 3D Q -tensor flow of liquid crystals based on the IEQ method. They proved the stability properties of the scheme and showed that it converges to weak solutions under a natural assumption. However, it seems that the maximum bound principle (MBP) can not be satisfied for their proposed schemes. Therefore, there is a high demand to construct efficient numerical schemes that can satisfy the unconditional energy dissipation law while preferably preserving the MBP with rigorous error estimates.

The main purpose of this paper is to construct efficient fully-discrete schemes for the Q -tensor flow using the stabilized exponential scalar auxiliary variable (sESAV) approach [16, 17, 25]. The main purposes of this paper are

- to construct two linear efficient fully discrete first- and second-order schemes for the Q -tensor flow of liquid crystals.
- to establish unconditional energy stability and prove the MBP for both two constructed schemes. Specifically, with an appropriate stabilizing parameter, the first-order scheme preserves the MBP unconditionally, while the second-order scheme does so with mild time-step size constraints.
- to carry out a rigorous error analysis for the fully discrete schemes, which is derived by establishing uniform bound for the numerical solution.

To the best of the authors' knowledge, this is the first linear, energy-stable and MBP-preserving numerical scheme for the Q -tensor flow in both 2D and 3D cases. Moreover, we also establish the rigorous error analysis for the proposed schemes by using the built-in stability results and a sequence of auxiliary estimates.

The remainder of the paper is structured as follows. Section 2 is devoted to the physical properties of the model and some preliminaries. In Section 3, we construct the fully-discrete first- and second-order scheme respectively, together with the energy dissipation law and MBP. In Section 4, we establish the rigorous error estimate for the numerical scheme. In Section 5, some numerical experiments are carried out to demonstrate the performance of the proposed schemes. Concluding remarks are given in Section 6.

2. The physical properties of the model and some preliminaries. In this section, we derive the energy dissipation law and MBP for the gradient flow (1.3) and give some preliminaries and notations below.

Firstly, we provide some notations. For any $\alpha \in \mathbb{R}$, α_+ and α_- are given by

$$(2.1) \quad \alpha_+ := \max\{0, \alpha\}, \quad \alpha_- := \max\{0, -\alpha\}.$$

For any tensor functions $\Phi, \Psi \in \mathbb{R}^{d \times d}$, we define the Frobenius product as follows:

$$\Phi : \Psi \stackrel{\text{def}}{=} \text{tr}(\Phi^T \Psi) = \sum_{i,j=1}^d \Phi^{i,j} \Psi^{i,j}.$$

The tensor function $\Phi \in \mathbb{R}^{d \times d}$, we use $|\Phi|_F$ to denote its Frobenius norm, i.e.,

$$|\Phi|_F = \sqrt{\text{tr}(\Phi^T \Phi)}.$$

Besides, we define $L^p (1 \leq p \leq \infty)$ tensor-function space by

$$L^p(\Omega \rightarrow \mathbb{R}^{d \times d}) \stackrel{\text{def}}{=} \{\Phi : \Omega \rightarrow \mathbb{R}^{d \times d}, |\Phi|_F \in L^p(\Omega)\}.$$

The corresponding L^∞ -norm for $\Phi \in L^p(\Omega \rightarrow \mathbb{R}^{d \times d})$ is given by

$$(2.2) \quad \|\Phi\|_{L^\infty(\Omega)} = \sup_{\mathbf{x} \in \Omega} |\Phi(\mathbf{x})|_F.$$

The gradient flow (1.3) satisfies the following energy dissipation law:

$$\frac{d}{dt} \mathcal{E}[Q] = - \int_{\Omega} \left| \frac{\delta \mathcal{E}}{\delta Q} - \lambda \mathbb{I}_d + \mu - \mu^T \right|^2 d\mathbf{x}.$$

Moreover, it has the nature of MBP property in the sense of the Frobenius norm, as stated in the following lemma.

Lemma 2.1 ([14, 21]) *Consider the evolution problem (1.3) with $a, b \in \mathbb{R}$ and $c > 0$ on a bounded, smooth domain $\Omega \subset \mathbb{R}^d$. For smooth solutions Q , there exists a positive number η such that, when $d = 2$ or $L_2 + L_3 = 0$ for $d = 3$, if $\|Q^0\|_{L^\infty(\Omega)} \leq \eta$, then it holds for any $T > 0$ and $t \in [0, T]$ that $\|Q(t)\|_{L^\infty(\Omega)} \leq \eta$.*

Proof. We first establish an a priori L^∞ -bound for the solution Q . Due to the fact that $c > 0$, there exists $\eta > 0$ such that for each $Q \in S^{(d)}$,

$$-a \text{tr}(Q^2) + b \text{tr}(Q^3) - c \text{tr}^2(Q^2) \leq 0, \quad \text{if } |Q| \geq \eta.$$

We assume $\|Q_0\|_{L^\infty(\Omega)} \leq \eta$, multiplying (1.4) by $Q(|Q|_F^2 - \eta^2)_+$ and integrating over Ω , after integration by parts, we obtain

$$\begin{aligned} & \frac{1}{4} \frac{d}{dt} \int_{\Omega} (|Q|_F^2 - \eta^2)_+^2 d\mathbf{x} \\ &= -L \int_{\Omega} |\nabla Q|^2 (|Q|_F^2 - \eta^2)_+ d\mathbf{x} - \frac{L}{2} \int_{\Omega} |\nabla (|Q|_F^2 - \eta^2)_+|^2 d\mathbf{x} \\ & \quad + \int_{\Omega} (-a \text{tr}(Q^2) + b \text{tr}(Q^3) - c \text{tr}^2(Q^2)) (|Q|_F^2 - \eta^2)_+ d\mathbf{x} \leq 0, \end{aligned}$$

which implies $\|Q(\cdot, t)\|_{L^\infty(\Omega)} \leq \eta$, $\forall t \in [0, T]$. □

Remark 2.1. For the 2D case, $Q \in \mathcal{S}^{(2)}$ implies $\text{tr}(Q^3) = 0$, then it follows from (1.2) and (1.4) that $b = 0$. Furthermore, we obtain the minimum value of η in Lemma 2.1 for $d = 2$, as follows:

$$(2.3) \quad \eta^{(2)} = \max \left\{ \|Q^0\|_{L^\infty(\Omega)}, \sqrt{\frac{a_-}{c}} \right\},$$

where a_- is defined in (2.1). As for the 3D case, we recall that $|\text{tr}(Q^3)| \leq |Q|_F^3 / \sqrt{6}$, which implies the minimum value of η for $d = 3$: (see e.g. [28, 5])

$$(2.4) \quad \eta^{(3)} = \begin{cases} \max \left\{ \|Q^0\|_{L^\infty(\Omega)}, \frac{|b| + \sqrt{b^2 - 24ac}}{2\sqrt{6c}} \right\}, & \text{if } a \leq \frac{b^2}{24c}, \\ \|Q^0\|_{L^\infty(\Omega)}, & \text{otherwise.} \end{cases}$$

From the definitions of (2.3) and (2.4), it also implies that $\|Q^0\|_{L^\infty(\Omega)} \leq \eta^{(d)}$, $d = 2, 3$.

3. Fully discrete sESAV schemes and structure-preserving properties.

In this section, we construct two efficient fully discrete schemes and establish the structure-preserving properties for the Q -tensor flow of liquid crystals by using the first- and second-order sESAV approach in time and finite difference method in space.

Recalling the Lemma 2.1 and noting the fact that $\mathcal{F}_{\text{bulk}}$ is bounded from below on $[-\eta, \eta]$, it holds that

$$(3.1) \quad -C_* \leq \mathcal{E}_1[Q(t)] = \int_{\Omega} \frac{a}{2} \text{tr}(Q^2) - \frac{b}{3} \text{tr}(Q^3) + \frac{c}{4} \text{tr}^2(Q^2) d\mathbf{x} \leq C^*,$$

for some constants $C_*, C^* \geq 0$.

Introducing $s(t) = \mathcal{E}_1[Q(t)]$ as an exponential scalar auxiliary variable, we then have the following energy form which is equivalent to $\mathcal{E}[Q]$

$$\begin{aligned} E[Q, s] &= \int_{\Omega} \left[\frac{L_1}{2} |\nabla Q|^2 + \frac{L_2 + L_3}{2} \sum_{i,j,k=1}^d \partial_j Q^{ij} \partial_k Q^{ik} \right] d\mathbf{x} + s \\ &= \int_{\Omega} \left[\frac{L_1}{2} |\nabla Q|^2 + \frac{L_2 + L_3}{2} \sum_{i=1}^d \left(\sum_{j=1}^d \partial_j Q^{ij} \right)^2 \right] d\mathbf{x} + s. \end{aligned}$$

We rewrite (1.4) as the following [17]:

$$(3.2a) \quad \partial_t Q^{ij} = L_1 \Delta Q^{ij} + \frac{L_2 + L_3}{2} \left(\sum_{k=1}^d (\partial_j \partial_k Q^{ik} + \partial_i \partial_k Q^{jk}) - \frac{2}{d} \sum_{k,l=1}^d \partial_l \partial_k Q^{lk} \delta^{ij} \right) + \frac{\exp\{s\}}{\exp\{\mathcal{E}_1[Q]\}} f(Q^{ij}),$$

$$(3.2b) \quad s_t = - \frac{\exp\{s\}}{\exp\{\mathcal{E}_1[Q]\}} \sum_{i,j=1}^d (f(Q^{ij}), Q_t^{ij}),$$

where

$$(3.3) \quad f(Q^{ij}) := -a Q^{ij} + b((Q^2)^{ij} - \frac{1}{d} \text{tr}(Q^2) \delta^{ij}) - c \text{tr}(Q^2) Q^{ij}.$$

3.1. Fully discrete sESAV finite difference schemes. To simplify the notation, we consider the problem (3.2) in the domain $\Omega = [0, L]^3$. Given a positive integer M , the uniform mesh partitioning size for each spatial direction is set to be $h = L/M$. We denote by \mathbb{E} and \mathbb{C} the two sets of mesh points, defined by

$$\mathbb{E} = \{x_p = ph \mid p = 0, 1, \dots, M\}, \quad \mathbb{C} = \{x_{p+\frac{1}{2}} = (p + \frac{1}{2})h \mid p = 0, 1, \dots, M-1\}.$$

The necessary grid function spaces are given by

$$\begin{aligned} \mathbb{E}_h^0 &= \{U : \mathbb{E} \times \mathbb{E} \times \mathbb{E} \rightarrow \mathbb{R} \mid U_{p,q,r}, U_{0,q,r} = U_{p,0,r} = U_{p,q,0} = 0, 0 \leq p, q, r \leq M\}, \\ e_h^{(1)} &= \{U : \mathbb{C} \times \mathbb{E} \times \mathbb{E} \rightarrow \mathbb{R} \mid U_{p+\frac{1}{2},q,r}, 0 \leq p \leq M-1, 0 \leq q, r \leq M\}, \\ e_h^{(2)} &= \{U : \mathbb{E} \times \mathbb{C} \times \mathbb{E} \rightarrow \mathbb{R} \mid U_{p,q+\frac{1}{2},r}, 0 \leq q \leq M-1, 0 \leq p, r \leq M\}, \\ e_h^{(3)} &= \{U : \mathbb{E} \times \mathbb{E} \times \mathbb{C} \rightarrow \mathbb{R} \mid U_{p,q,r+\frac{1}{2}}, 0 \leq p, q \leq M, 1 \leq r \leq M-1\}. \end{aligned}$$

For ease of notation, we will also impose homogenous Dirichlet boundary condition on the ghost nodes, that is, for any $-1 \leq p, q, r \leq M + 1$,

$$U_{-1,q,r} = U_{M+1,q,r} = U_{p,-1,r} = U_{p,M+1,r} = U_{p,q,-1} = U_{p,q,M+1} = 0.$$

Then, we give several difference operators for the grid function $\{U_{p,q,r}\}_{p,q,r=0}^M$:

$$\begin{aligned} (D_1^+ U)_{p+\frac{1}{2},q,r} &= \frac{U_{p+1,q,r} - U_{p,q,r}}{h}, \quad (D_2^+ U)_{p,q+\frac{1}{2},r} = \frac{U_{p,q+1,r} - U_{p,q,r}}{h}, \\ (D_3^+ U)_{p,q,r+\frac{1}{2}} &= \frac{U_{p,q,r+1} - U_{p,q,r}}{h}, \quad (D_1^- U)_{p,q,r} = \frac{U_{p+\frac{1}{2},q,r} - U_{p-\frac{1}{2},q,r}}{h}, \\ (D_2^- U)_{p,q,r} &= \frac{U_{p,q+\frac{1}{2},r} - U_{p,q-\frac{1}{2},r}}{h}, \quad (D_3^- U)_{p,q,r} = \frac{U_{p,q,r+\frac{1}{2}} - U_{p,q,r-\frac{1}{2}}}{h}, \\ (D_1^c U)_{p,q,r} &= \frac{U_{p+1,q,r} - U_{p-1,q,r}}{2h}, \quad (D_2^c U)_{p,q,r} = \frac{U_{p,q+1,r} - U_{p,q-1,r}}{2h}, \\ (D_3^c U)_{p,q,r} &= \frac{U_{p,q,r+1} - U_{p,q,r-1}}{2h}. \end{aligned}$$

Moreover, we denote by $D_{k,l}^c U = D_k^c D_l^c U$, $k, l = 1, 2, 3$ for simplicity. The discrete gradient operator $\nabla_h: E_h^0 \rightarrow (e_h^{(1)}, e_h^{(2)}, e_h^{(3)})^T$ is given by

$$(\nabla_h U)_{p,q,r} = \left((D_1^+ U)_{p+\frac{1}{2},q,r}, (D_2^+ U)_{p,q+\frac{1}{2},r}, (D_3^+ U)_{p,q,r+\frac{1}{2}} \right)^T,$$

and the discrete divergence operator $\nabla_h: (e_h^{(1)}, e_h^{(2)}, e_h^{(3)})^T \rightarrow E_h^0$ is represented by

$$\nabla_h \cdot (U^{(1)}, U^{(2)}, U^{(3)})^T = D_1^- U^{(1)} + D_2^- U^{(2)} + D_3^- U^{(3)},$$

where $(U^{(1)}, U^{(2)}, U^{(3)})^T \in (e_h^{(1)}, e_h^{(2)}, e_h^{(3)})$. Therefore, the discrete Laplacian $\Delta_h: E_h^0 \rightarrow E_h^0$ is defined by

$$\Delta_h U = \nabla_h \cdot (\nabla_h U)$$

for any grid function $U \in E_h^0$. We also introduce several discrete inner products:

$$\begin{aligned} \langle U, V \rangle_h &= h^3 \sum_{p,q,r=1}^{M-1} U_{p,q,r} V_{p,q,r}, \quad \forall U, V \in E_h^0, \\ [U^{(k)}, V^{(k)}]_{k,h} &= \langle a_k(U^{(k)} V^{(k)}), 1 \rangle_h, \quad \forall U^{(k)}, V^{(k)} \in e_h^{(k)}, \quad k = 1, 2, 3, \\ [(U^{(1)}, U^{(2)}, U^{(3)})^T, (V^{(1)}, V^{(2)}, V^{(3)})^T]_h &= \sum_{k=1}^3 [U^{(k)}, V^{(k)}]_{k,h}, \end{aligned}$$

where $a_k: e_h^k \rightarrow E_h^0$, $k = 1, 2, 3$ are three average operators, defined by

$$\begin{aligned} (a_1 U^{(1)})_{p,q,r} &= \frac{1}{2}(U_{p+\frac{1}{2},q,r}^{(1)} + U_{p-\frac{1}{2},q,r}^{(1)}), \quad (a_2 U^{(2)})_{p,q,r} = \frac{1}{2}(U_{p,q+\frac{1}{2},r}^{(2)} + U_{p,q-\frac{1}{2},r}^{(2)}), \\ (a_3 U^{(3)})_{p,q,r} &= \frac{1}{2}(U_{p,q,r+\frac{1}{2}}^{(3)} + U_{p,q,r-\frac{1}{2}}^{(3)}), \quad 0 \leq p, q, r \leq M \end{aligned}$$

for any $U^{(k)} \in e_h^k$, $k = 1, 2, 3$. Then, for any $U \in \mathbb{E}_h^0$, the corresponding discrete L^2 , H^1 and L^∞ norms are given by

$$\begin{aligned} \|U\|_h^2 &= \langle U, U \rangle_h, \quad \|\nabla_h U\|_h^2 = [\nabla_h U, \nabla_h U]_h = \sum_{k=1}^3 [D_k^+ U, D_k^+ U]_{k,h}, \\ \|U\|_{H_h^1}^2 &= \|U\|_h^2 + \|\nabla_h U\|_h^2, \quad \|U\|_\infty = \max_{0 \leq p \leq M} \sum_{p,r=0}^M |U_{p,q,r}|. \end{aligned}$$

Using the summation-by-parts, it is easy to check that, for any $U, V \in \mathbb{E}_h^0$, it holds

$$(3.4) \quad \begin{aligned} \langle D_k^- D_k^+ U, V \rangle_h &= -\langle D_k^+ U, D_k^- V \rangle_h = \langle U, D_k^- D_k^+ V \rangle_h, \\ \langle D_{k,l}^c U, V \rangle_h &= -\langle D_l^c U, D_k^c V \rangle_h = -\langle D_k^c U, D_l^c V \rangle_h = \langle U, D_{k,l}^c V \rangle_h, \end{aligned}$$

which also imposes that

$$\langle \Delta_h U, V \rangle_h = -[\nabla_h U, \nabla_h V] = \langle U, \Delta_h V \rangle_h.$$

Analogous to the tensor-function space $\mathcal{S}^{(d)}$ in (1.1), we also define grid tensor-function space satisfying the homogenous Dirichlet boundary condition for $d = 3$,

$$\mathbb{S}_h^{(3)} = \left\{ \Phi_h \mid \Phi_h^{i,j} \in \mathbb{E}_h^0, \operatorname{tr}(\Phi_h) := \sum_{i=1}^3 \Phi_h^{ii} = 0, \Phi_h^{i,j} = \Phi_h^{j,i}, i, j = 1, 2, 3 \right\}.$$

We can give a similar definition of general tensor-function space \mathbb{S}^d for $d = 2$. Then, the corresponding discrete L^2 norm and the discrete H^1 semi-norm of the grid tensor-functions $\Phi_h, \Psi_h \in \mathbb{S}_h^{(3)}$, are defined respectively by

$$\|\Phi_h\|_h := \sqrt{\sum_{i,j=1}^3 \|\Phi_h^{i,j}\|_h^2}, \quad \|\nabla_h \Phi_h\|_h := \sqrt{\sum_{i,j}^3 \|\nabla_h \Phi_h^{i,j}\|_h^2}.$$

Moreover, we define following tensor-matrix-product and discrete Frobenius-product for any $\Phi_h, \Psi_h \in \mathbb{S}_h^{(3)}$, respectively, by

$$(\Phi_h \Psi_h)^{i,j} := \sum_{k=1}^3 \Phi_h^{i,k} \cdot * \Psi_h^{k,j}, \quad i, j = 1, 2, 3; \quad \Phi_h : \Psi_h := \operatorname{tr}(\Phi_h \Psi_h) = \sum_{i,j=1}^3 \Phi_h^{i,j} \cdot * \Psi_h^{i,j},$$

where $\Phi_h^{i,k} \cdot * \Psi_h^{k,j}$ represents the point-wise multiplication of matrices, that is

$$(\Phi_h^{i,k} \cdot * \Psi_h^{k,j})_{p,q,r} = (\Phi_h^{i,k})_{p,q,r} \cdot (\Psi_h^{k,j})_{p,q,r}, \quad p, q, r = 0, 1, \dots, M.$$

Now, we are ready to construct the semi-discrete problem of (3.2): to find $Q_h(t) \in \mathbb{S}_h$ and $s(t)$ for $t > 0$ satisfying

$$(3.5a) \quad \frac{dQ_h^{ij}}{dt} = L_1 \Delta_h Q_h^{ij} + \frac{L_2 + L_3}{2} \mathcal{D}_h^c Q_h^{ij} + g(Q_h, s) f(Q_h^{ij}),$$

$$(3.5b) \quad s_t = -g(Q_h, s) \sum_{i,j=1}^3 \langle f(Q_h^{ij}), \frac{dQ_h^{ij}}{dt} \rangle_h,$$

where $g(Q_h, s_h) := \exp\{s_h\} / \exp\{\mathcal{E}_{1h}[Q_h]\} > 0$, $\mathcal{E}_{1h}[Q_h] := \langle \frac{a}{2} \operatorname{tr}(Q_h^2) - \frac{b}{3} \operatorname{tr}(Q_h^3) + \frac{c}{4} \operatorname{tr}^2(Q_h^2), 1 \rangle_h$, and

$$(3.6) \quad \mathcal{D}_h^c Q_h^{ij} := \sum_{k=1}^3 (D_{jk}^c Q_h^{ik} + D_{ik}^c Q_h^{jk}) - \frac{2}{3} \sum_{k,l=1}^3 D_{lk}^c Q_h^{lk} \delta^{ij}.$$

Taking the discrete inner product of equation (3.5a) with $dQ_h^{i,j}/dt$, using the identity (3.4), summing them up for i, j from 1 to 3, and together with (3.5b), we derive that

$$\frac{d}{dt} E[Q_h, s_h] = -\left\| \frac{dQ_h}{dt} \right\|_h^2,$$

where the discrete energy is given by

$$(3.7) \quad E_h[Q_h, s] = \frac{L_1}{2} \|\nabla_h Q_h\|_h^2 + \frac{L_2 + L_3}{2} \sum_{i=1}^3 \|D_1^c Q_h^{i1} + D_2^c Q_h^{i2} + D_3^c Q_h^{i3}\|_h^2 + s,$$

which is an approximation of the original discrete energy $\mathcal{E}[Q]$.

Now, we are in a position to construct fully discrete first- and second-order in-time schemes for the Q-tensor model (1.3). The first-order stabilized ESAV (sESAV1) fully-discrete scheme for (3.5) reads: given the initial values of (Q_h^0, s^0) , then for any $n \geq 0$, we find $(Q_h^{n+1}, s^{n+1}) \in \mathbb{S}_h^{(3)} \times \mathbb{R}$ such that for $i, j = 1, 2, 3$

$$(3.8a) \quad \frac{Q_h^{ij,n+1} - Q_h^{ij,n}}{\tau} = L_1 \Delta_h Q_h^{ij,n+1} + \frac{L_2 + L_3}{2} \mathcal{D}_h^c Q_h^{ij,n+1} + g(Q_h^n, s^n) (f(Q_h^{ij,n}) - \kappa(Q_h^{ij,n+1} - Q_h^{ij,n})),$$

$$(3.8b) \quad \frac{s^{n+1} - s^n}{\tau} = -g(Q_h^n, s^n) \sum_{i,j=1}^3 \left\langle f(Q_h^{ij,n}), \frac{Q_h^{ij,n+1} - Q_h^{ij,n}}{\tau} \right\rangle_h,$$

where $\kappa \geq 0$ is a stabilizing constant and the operator $\mathcal{D}_h^c Q_h^{ij,n+1}$ is given in (3.6). We denote the above first-order scheme as $[Q_h^{n+1}, s^{n+1}] = \text{sESAV1}(Q_h^n, s^n, \tau)$. We point out that the constructed scheme (3.8) preserves the trace-free and symmetry property of Q , which can be obtained by using a similar proof in [8].

Proposition 3.1 *If Q^n is trace-free and symmetric, then Q_h^{n+1} computed by the sESAV1 scheme (3.8) is also trace-free and symmetric.*

The unconditionally energy stability of the sESAV1 scheme (3.8) is stated in the following theorem.

Theorem 3.2 *For any $\kappa \geq 0$, the sESAV1 scheme (3.8) is unconditionally energy stable in the sense that*

$$E_h[Q_h^{n+1}, s^{n+1}] \leq E_h[Q_h^n, s^n], \quad n \geq 0.$$

Moreover, it holds that $s^n \leq E_h[Q_h^0, \mathcal{E}_{1,h}[Q_h^0]]$.

Proof. Taking the discrete inner product with (3.8a) by $Q_h^{ij,n+1} - Q_h^{ij,n}$, using the discrete integral by parts (3.4) and summing up i, j from 1 to 3, yields

$$(3.9) \quad \begin{aligned} & \left(\frac{1}{\tau} + \kappa g(Q_h^n, s^n) \right) \|Q_h^{n+1} - Q_h^n\|_h^2 \\ & \leq -\frac{L_1}{2} (\|\nabla_h Q_h^{n+1}\|_h^2 - \|\nabla_h Q_h^n\|_h^2) + \sum_{i,j=1}^3 \langle \mathcal{D}_h^c Q_h^{ij,n+1}, Q_h^{ii,n+1} - Q_h^{ii,n} \rangle_h \\ & \quad + g(Q_h^n, s^n) \sum_{i,j=1}^3 \langle f(Q_h^{ij,n}), Q_h^{ij,n+1} - Q_h^{ij,n} \rangle_h. \end{aligned}$$

Moreover, we use (3.4) and $Q_h^{ij} = Q_h^{ji}$ for $i, j = 1, 2, 3$, to obtain that

$$\begin{aligned}
 (3.10) \quad & \sum_{i,j=1}^3 \left\langle \sum_{k=1}^3 (D_{jk}^c Q_h^{ik,n+1} + D_{ik}^c Q_h^{jk,n+1}), Q_h^{ij,n+1} - Q_h^{ij,n} \right\rangle_h \\
 & = -2 \sum_{i=1}^3 \left\langle \sum_{k=1}^3 D_k^c Q_h^{ik,n+1}, \sum_{k=1}^3 D_k^c (Q_h^{ik,n+1} - Q_h^{ik,n}) \right\rangle_h \\
 & \leq - \sum_{i=1}^3 \left[\left\| \sum_{k=1}^3 D_k^c Q_h^{ik,n+1} \right\|_h^2 - \left\| \sum_{k=1}^3 D_k^c Q_h^{ik,n} \right\|_h^2 \right].
 \end{aligned}$$

In addition, using the trace-free preservation of the sESAV1 scheme (3.8), we derive

$$(3.11) \quad \sum_{i,k,l=1}^3 \left\langle D_{lk}^c Q_h^{lk,n+1}, Q_h^{ii,n+1} - Q_h^{ii,n} \right\rangle_h = 0$$

It follows from (3.8b)-(3.10) and (3.11) that

$$E_h[Q_h^{n+1}, s^{n+1}] - E_h[Q_h^n, s^n] = -\left(\frac{1}{\tau} + \kappa g(Q_h^n, s^n)\right) \|Q_h^{n+1} - Q_h^n\|_h^2 \leq 0.$$

Noting that $s^0 = \mathcal{E}_{1,h}[Q_h^0]$, we have

$$(3.12) \quad s^n \leq E_h[Q_h^n, s^n] \leq E_h[Q_h^{n-1}, s^{n-1}] \leq \dots \leq E_h[Q_h^0, s^0] = E_h[Q_h^0, \mathcal{E}_{1,h}[Q_h^0]]. \quad \square$$

The second-order in time stabilized ESAV (sESAV2) fully-discrete scheme for the semi-discrete problem (3.5) is presented as follows: given the initial values of (Q_h^0, s^0) , then for any $n \geq 0$, we obtain $(Q_h^{n+1}, s^{n+1}) \in \mathbb{S}_h^3 \times \mathbb{R}$ through the following

$$\begin{aligned}
 (3.13a) \quad \frac{Q_h^{ij,n+1} - Q_h^{ij,n}}{\tau} & = L_1 \Delta_h Q_h^{ij,n+\frac{1}{2}} + \mathcal{D}_h^c Q_h^{ij,n+\frac{1}{2}} \\
 & + g(Q_{*,h}^{n+\frac{1}{2}}, s_*^{n+\frac{1}{2}}) (f(Q_{*,h}^{ij,n+\frac{1}{2}}) - \kappa(Q_h^{ij,n+\frac{1}{2}} - Q_{*,h}^{ij,n+\frac{1}{2}})),
 \end{aligned}$$

$$\begin{aligned}
 (3.13b) \quad \frac{s^{n+1} - s^n}{\tau} & = -g(Q_{*,h}^{n+\frac{1}{2}}, s_*^{n+\frac{1}{2}}) \sum_{i,j=1}^3 \left\langle f(Q_{*,h}^{ij,n+\frac{1}{2}}), \frac{Q_h^{ij,n+1} - Q_h^{ij,n}}{\tau} \right\rangle_h \\
 & + \kappa g(Q_{*,h}^{n+\frac{1}{2}}, s_*^{n+\frac{1}{2}}) \sum_{i,j=1}^3 \left\langle Q_h^{ij,n+\frac{1}{2}} - Q_{*,h}^{ij,n+\frac{1}{2}}, \frac{Q_h^{ij,n+1} - Q_h^{ij,n}}{\tau} \right\rangle_h.
 \end{aligned}$$

where the operator \mathcal{D}_h^c is defined in (3.6) and $Q_h^{ij,n+1/2} := (Q_h^{ij,n+1} + Q_h^{ij,n})/2$ for $i, j = 1, 2, 3$. Here, $Q_{*,h}^{n+\frac{1}{2}}$ and $s_*^{n+\frac{1}{2}}$ are updated by the sESAV1 scheme (3.8), that is $[Q_{*,h}^{n+\frac{1}{2}}, s_*^{n+\frac{1}{2}}] = \text{sESAV1}(Q_h^n, s^n, \tau/2)$.

Using a similar approach reported in [8], we can deduce that the above scheme also maintains the trace-free and symmetry properties of Q . Moreover, it is unconditionally stable in the sense of a modified energy, as stated in the following theorem. The proof is similar to that of Theorem 3.2, so we omit it here and leave it for interested readers.

Theorem 3.3 *For any $\kappa \geq 0$, the sESAV2 scheme is unconditionally energy-dissipative in the sense that*

$$E_h[Q_h^{n+1}, s^{n+1}] \leq E_h[Q_h^n, s^n], \quad n \geq 0.$$

Moreover, it holds that $s^n \leq E_h[Q_h^0, \mathcal{E}_{1,h}[Q_h^0]]$ and $s_*^{n+\frac{1}{2}} \leq E_h[Q_h^0, \mathcal{E}_{1,h}[Q_h^0]]$.

3.2. The discrete maximum bound principle. As stated in Lemma 2.1, the MBP property of Q in Frobenius-norm holds for the Q-tensor model (1.3) in cases of $d = 2$ and $d = 3$ with $L_2 + L_3 = 0$. For these two cases, the sESAV1 scheme (3.8) can be rewritten as follows: Given the initial values of (Q_h^0, s^0) , to find $(Q_h^{n+1}, s^{n+1}) \in \mathbb{S}_h^{(d)} \times \mathbb{R}$, $d = 2, 3$, $n \geq 0$, such that

$$(3.14a) \quad G_h Q_h^{ij,n+1} = \frac{1}{\tau} Q_h^{ij,n} + g(Q_h^n, s^n) [\kappa Q_h^{ij,n} + f(Q_h^{ij,n})],$$

$$(3.14b) \quad s^{n+1} = s^n - g(Q_h^n, s^n) \sum_{i,j=1}^3 \left\langle f(Q_h^{ij,n}), Q_h^{ij,n+1} - Q_h^{ij,n} \right\rangle_h.$$

with $G_h := \left(\left(\frac{1}{\tau} + \kappa g(Q_h^n, s^n) \right) I - L \Delta_h \right)$ and $L = L_1 + \frac{L_2 + L_3}{2}$, where we have used the fact that, for the tensor-function $Q \in \mathcal{S}^{(2)}$, it holds

$$\sum_{k=1}^2 (\partial_j \partial_k Q^{ik} + \partial_i \partial_k Q^{jk}) - \sum_{k,l=1}^2 \partial_l \partial_k Q^{lk} \delta^{ij} = \Delta Q^{ij}, \quad i, j = 1, 2.$$

For convenience, we will denote the first-order scheme (3.14) as $[Q_h^{n+1}, s^{n+1}] = \text{MBP-sESAV1}(Q_h^n, s^n, \tau)$. Furthermore, we can rewrite MBP-sESAV1 scheme (3.14) in vector form for $d = 2, 3$, as follows:

$$(3.15a) \quad \mathbb{G}_h \vec{Q}_h^{ij,n+1} = \frac{1}{\tau} \vec{Q}_h^{ij,n} + g(Q_h^n, s^n) [\kappa \vec{Q}_h^{ij,n} + f(\vec{Q}_h^{ij,n})],$$

$$(3.15b) \quad s^{n+1} = s^n - g(Q_h^n, s^n) \sum_{i,j=1}^3 \left\langle f(\vec{Q}_h^{ij,n}), \vec{Q}_h^{ij,n+1} - \vec{Q}_h^{ij,n} \right\rangle_h.$$

where $\mathbb{G}_h := ((1/\tau + \kappa g(Q_h^n, s^n))I - LD_h)$, and $\vec{Q}_h^{ij,n} \in \mathbb{R}^{(M+1)^d}$ is the vector representation of $Q_h^{ij,n} \in \mathbb{S}_h^0$, with the elements organized in the order of the x_1, \dots, x_d directions. Here $f(\vec{Q}_h^{ij,n}) \in \mathbb{R}^{(M+1)^d}$ represents the element-wise function of $\vec{Q}_h^{ij,n}$ and tensor form D_h of the discrete Δ_h is given by

$$(3.16) \quad D_h = \begin{cases} I \otimes \Lambda_h + \Lambda_h \otimes I, & \text{for } d = 2; \\ I \otimes I \otimes \Lambda_h + I \otimes \Lambda_h \otimes I + \Lambda_h \otimes I \otimes I, & \text{for } d = 3. \end{cases}$$

with I denoting the identity matrix (with the matched dimensions) and

$$\Lambda_h = \frac{1}{h^2} \begin{pmatrix} -2 & 1 & & & \\ 1 & -2 & 1 & & \\ & \ddots & \ddots & \ddots & \\ & & 1 & -2 & 1 \\ & & & 1 & -2 \end{pmatrix}_{(M+1) \times (M+1)},$$

Moreover, we denote by $\vec{Q}_h := [\vec{Q}_h^{11}, \dots, \vec{Q}_h^{1d}; \dots; \vec{Q}_h^{d1}, \dots, \vec{Q}_h^{dd}]$ the vector form of the grid tensor-function $Q_h \in \mathbb{S}_h^{(d)}$ for $d = 2, 3$. Analogous to the Frobenius-norm and the L^∞ -norm for tensor function $Q \in L^p(\Omega \rightarrow \mathbb{R}^{d \times d})$, the discrete Frobenius-norm and L^∞ -Frobenius-norm for the grid tensor-function \vec{Q}_h are given respectively by

$$|\vec{Q}_h|_F^2 = \sum_{i,j}^d \left(\vec{Q}_h^{ij} \right)^{*2}, \quad \|\vec{Q}_h\|_{F,\infty} = \left\| |\vec{Q}_h|_F \right\|_\infty,$$

where $(\vec{Q}_h^{ij})^{*2} := \vec{Q}_h^{ij} \cdot * \vec{Q}_h^{ij}$. Before investigating the MBP preservation of the proposed scheme (3.14), we first review some useful lemmas.

Lemma 3.4 [4, 11, 24] *Let $B = (b_{kl})$ be a real $N \times N$ matrix and $A = \alpha I - B$ with $\alpha > 0$. If B is a negative diagonally dominant matrix, i.e.*

$$(3.17) \quad b_{kk} \leq 0 \quad \text{and} \quad b_{kk} + \sum_{l \neq k} |b_{kl}| \leq 0, \quad 1 \leq k \leq N,$$

then, A is invertible and satisfies $\|A^{-1}\|_\infty \leq 1/\alpha$. Furthermore, if $b_{k,l} \geq 0$ for $k \neq l$ and $1 \leq k, l \leq N$, then it holds $A^{-1} \geq 0$, which means that all the elements of A^{-1} are non-negative.

Lemma 3.5 *Assume $A := (a_{kl} \geq 0)$ is a real non-negative $N \times N$ matrix, and $\vec{\Phi}^{ij}$, $i, j = 1, \dots, d$ are real $N \times 1$ vectors. Then, it holds*

$$\sqrt{\sum_{i,j=1}^d (A\vec{\Phi}^{ij})^{*2}} \leq A \sqrt{\sum_{i,j=1}^d (\vec{\Phi}^{ij})^{*2}}.$$

Proof. The well-known Minkowski inequality is stated as follows:

$$\left(\sum_{k=1}^m |x_k + y_k|^p \right)^{\frac{1}{p}} \leq \left(\sum_{k=1}^m |x_k|^p \right)^{\frac{1}{p}} + \left(\sum_{k=1}^m |y_k|^p \right)^{\frac{1}{p}}, \quad 1 \leq p < \infty$$

for any real numbers x_i, y_i , $(i = 1, \dots, m)$. Then, using it with $p = 2$ for m_1 times, we can deduce that

$$(3.18) \quad \left(\sum_{l=1}^{m_2} \left(\sum_{k=1}^{m_1} \alpha_k^l \right)^2 \right)^{\frac{1}{2}} \leq \sum_{k=1}^{m_1} \left(\sum_{l=1}^{m_2} (\alpha_k^l)^2 \right)^{\frac{1}{2}}.$$

Let the $N \times 1$ vectors $\vec{b} := \sqrt{\sum_{i,j=1}^d (A\vec{\Phi}^{ij})^{*2}}$ and $\vec{c} := \sqrt{\sum_{i,j=1}^d (\vec{\Phi}^{ij})^{*2}}$. Then, using (3.18), we deduce that

$$(3.19) \quad \vec{b}_k = \sqrt{\sum_{i,j=1}^d \left(\sum_{l=1}^N a_{kl} \vec{Q}_l^{ij} \right)^2} \leq \sum_{l=1}^N \sqrt{\sum_{i,j=1}^d a_{k,l}^2 (\vec{Q}_l^{ij})^2} = \sum_{l=1}^N a_{k,l} \sqrt{\sum_{i,j=1}^d (\vec{Q}_l^{ij})^2} = \vec{c}_k,$$

for $1 \leq k \leq N$, which completes the proof. \square

Lemma 3.6 *For any $Q \in \mathcal{S}^{(d)}$, $d = 2, 3$, assume that $\|Q\|_{L^\infty(\Omega)} \leq \eta^{(d)}$ and $\kappa \geq \max\{a + c(\eta^{(d)})^2, 0\}$ with $\eta^{(d)}$ defined in (2.3) and (2.4), then it holds that*

$$(3.20) \quad \sqrt{\sum_{i,j=1}^d (\kappa Q^{ij} + f(Q^{ij}))^2} \leq \kappa |Q|_F + \bar{f}(|Q|_F)$$

with the function $\bar{f}(\cdot)$ defined by

$$(3.21) \quad \bar{f}(\xi) = -a\xi + \frac{b}{\sqrt{6}}\xi^2 - c\xi^3,$$

where $b = 0$ for $d = 2$ as discussed in Remark 2.1.

Proof. For the 2D case, we use $\kappa \geq \max\{a + c(\eta^{(2)})^2, 0\}$, $\|Q\|_{L^\infty(\Omega)} \leq \eta^{(2)}$ and the definition of $f(\cdot)$ in (3.3) to obtain that

$$\begin{aligned} \sqrt{\sum_{i,j=1}^d (\kappa Q^{ij} + f(Q^{ij}))^2} &= \sqrt{(\kappa - a - c \operatorname{tr}(Q^2))^2 \sum_{i,j=1}^d (Q^{ij})^2} \\ &= (\kappa - a - c|Q|_F^2)|Q|_F = \kappa|Q|_F + \bar{f}(|Q|_F). \end{aligned}$$

Then we obtain the desired result for $d = 2$.

For the 3D case, it holds

$$\begin{aligned} (3.22) \quad & \sqrt{\sum_{i,j=1}^d (\kappa Q^{ij} + f(Q^{ij}))^2} \\ & \leq \sqrt{(\kappa - a - c \operatorname{tr}(Q^2))^2 \sum_{i,j=1}^d (Q^{ij})^2} + \sqrt{\sum_{i,j=1}^d b^2 ((Q^2)^{ij} - \frac{1}{3} \operatorname{tr}(Q) \delta^{ij})^2} \\ & = (\kappa - a - c|Q|_F^2)|Q|_F + b \left| Q^2 - \frac{1}{3} \operatorname{tr}(Q^2) I \right|_F, \end{aligned}$$

where we have used $\kappa \geq \max\{a + c(\eta^{(3)})^2, 0\}$ and $\|Q\|_{L^\infty(\Omega)} \leq \eta^{(3)}$. Since the tensor-function $Q \in \mathcal{S}^{(3)}$, then we can write $Q = P^T AP$ with $P^T P = I$ and $A = \operatorname{diag}(\lambda_1, \lambda_2, \lambda_3)$ being a diagonal matrix with $\lambda_3 = -\lambda_1 - \lambda_2$. Furthermore, it follows from $Q^2 = P^T A^2 P$ and $\operatorname{tr}(Q^2) = \operatorname{tr}(A^2)$ that,

$$\begin{aligned} (3.23) \quad & |Q^2 - \frac{1}{3} \operatorname{tr}(Q^2) I|_F = |A^2 - \frac{1}{3} \operatorname{tr}(A^2) I|_F \\ & = \frac{1}{3} \sqrt{(2\lambda_1^2 - \lambda_2^2 - \lambda_3^2)^2 + (-\lambda_1^2 + 2\lambda_2^2 - \lambda_3^2)^2 + (-\lambda_1^2 - \lambda_2^2 + 2\lambda_3^2)^2} \\ & = \frac{1}{\sqrt{6}} [\lambda_1^2 + \lambda_2^2 + (\lambda_1 + \lambda_2)^2] = \frac{1}{\sqrt{6}} |Q|_F^2, \end{aligned}$$

where we have used

$$\lambda_1^2 \lambda_2^2 + \lambda_1^2 \lambda_3^2 + \lambda_2^2 \lambda_3^2 = \frac{1}{2} [\lambda_1^4 + \lambda_2^4 + (\lambda_1 + \lambda_2)^4] = \frac{1}{4} (\lambda_1^2 + \lambda_2^2 + (\lambda_1 + \lambda_2)^2)^2.$$

Combining (3.22) and (3.23) gives the desired result (3.20) for $d = 3$. \square

Remark 3.1. For the 2D case ($b = 0$), we have $\bar{f}(\xi) = (-a - c\xi^2)\xi$ from (3.21). Thus, it follows from $c > 0$ and the definition of $\eta^{(2)} \geq \sqrt{\frac{a}{c}}$ in (2.3) that $\bar{f}(\eta^{(2)}) \leq 0$. Similarly, we can deduce that $\bar{f}(\eta^{(3)}) \leq 0$ for the 3D case.

Lemma 3.7 *Assume $\kappa \geq \max_{\xi \in [0, \eta^{(d)}]} |\bar{f}'(\xi)|$ with $\eta^{(d)}$ and $g(\cdot)$ defined in (2.4) and (3.21), respectively. Then it holds that*

$$(3.24) \quad |\kappa\xi + \bar{f}(\xi)| \leq \kappa\eta^{(d)}, \quad \forall \xi \in [0, \eta^{(d)}].$$

Proof. Setting $h(\xi) = \kappa\xi + \bar{f}(\xi)$ and using $\kappa \geq \max_{\xi \in [0, \eta^{(d)}]} |\bar{f}'(\xi)|$, we have for $\xi \in [0, \eta^{(d)}]$,

$$h'(\xi) = \kappa - \bar{f}'(\xi) \geq 0.$$

Together with $h(0) = 0$ and $h(\eta^{(d)}) = \kappa\eta^{(d)} + \bar{f}(\eta^{(d)}) \leq \kappa\eta^{(d)}$, we obtain (3.24). \square

Theorem 3.8 For $\eta^{(d)}$ defined in (2.3) and (2.4), assume that the stabilizing parameter κ satisfies

$$(3.25) \quad \kappa \geq \max \{a + c(\eta^{(d)})^2, \max_{\xi \in [0, \eta^{(d)}]} |\bar{f}'(\xi)|\}.$$

Then, the MBP-sESAV1 scheme (3.14) unconditionally preserves the MBP for $\{Q_h^n\}$:

$$(3.26) \quad \|\vec{Q}_h^n\|_{F,\infty} \leq \eta^d, \quad \forall n \geq 0.$$

Proof. It follows from the definition of $\eta^{(d)}$ in (2.3) and (2.4) that $\|\vec{Q}_h^0\|_{F,\infty} \leq \eta^{(d)}$. We suppose $\|\vec{Q}_h^k\|_{F,\infty} \leq \eta^{(d)}$ for any $0 \leq k \leq n$, which also implies that $0 \leq |\vec{Q}_h^k|_F \leq \eta^{(d)}$ for $0 \leq k \leq n$. Next, we will show $\|\vec{Q}_h^{n+1}\|_{F,\infty} \leq \eta^{(d)}$. From (3.15), we have

$$(3.27) \quad \vec{Q}_h^{ij,n+1} = \mathbb{G}_h^{-1} \left(\frac{1}{\tau} \vec{Q}_h^{ij,n} + g(Q_h^n, s^n) [\kappa \vec{Q}_h^{ij,n} + f(\vec{Q}_h^{ij,n})] \right),$$

Furthermore, we use the above equality, the definition of \mathbb{G}_h , Lemmas 3.4-3.6 to obtain

$$\begin{aligned} |\vec{Q}_h^{n+1}|_F &= \sqrt{\sum_{i,j=1}^d (\vec{Q}_h^{ij,n+1})^{*2}} \\ &= \sqrt{\sum_{i,j=1}^d \left[\mathbb{G}_h^{-1} \left(\frac{1}{\tau} \vec{Q}_h^{ij,n} + g(Q_h^n, s^n) [\kappa \vec{Q}_h^{ij,n} + f(\vec{Q}_h^{ij,n})] \right) \right]^{*2}} \\ &\leq \mathbb{G}_h^{-1} \left[\frac{1}{\tau} \sqrt{\sum_{i,j=1}^d (\vec{Q}_h^{ij,n})^{*2}} + g(Q_h^n, s^n) \sqrt{\sum_{i,j=1}^d [\kappa \vec{Q}_h^{ij,n} + f(\vec{Q}_h^{ij,n})]^{*2}} \right] \\ &\leq \mathbb{G}_h^{-1} \left[\frac{1}{\tau} |\vec{Q}_h^n|_F + g(Q_h^n, s^n) [\kappa |\vec{Q}_h^n|_F + \bar{f}(|\vec{Q}_h^n|_F)] \right]. \end{aligned}$$

Thus, together with Lemma 3.4 and Lemma 3.7, we derive

$$\begin{aligned} \|\vec{Q}_h^{n+1}\|_F &\leq \left\| \mathbb{G}_h^{-1} \left[\frac{1}{\tau} |\vec{Q}_h^n|_F + g(Q_h^n, s^n) [\kappa |\vec{Q}_h^n|_F + \bar{f}(|\vec{Q}_h^n|_F)] \right] \right\|_\infty \\ &\leq \|\mathbb{G}_h^{-1}\|_\infty \left[\frac{1}{\tau} \|\vec{Q}_h^n\|_{F,\infty} + g(Q_h^n, s^n) \|\kappa |\vec{Q}_h^n|_F + \bar{f}(|\vec{Q}_h^n|_F)\|_\infty \right] \\ &\leq \left(\frac{1}{\tau} + \kappa g(Q_h^n, s^n) \right)^{-1} \left(\frac{1}{\tau} + \kappa g(Q_h^n, s^n) \right) \eta^{(d)} = \eta^{(d)}, \end{aligned}$$

which completes the proof. \square

With a similar proving process of Corollary 3.5 in [16], we can derive the following corollary directly.

Corollary 3.9 For fixed h and $\eta^{(d)}$ defined in (2.3) and (2.4), if the stabilizing parameter κ satisfies the condition (3.25), then there exist two constants $G_* > 0$ and $G^* > 0$ such that

$$G_* < g(Q_h^k, s^k) \leq G^*, \quad n \geq 0.$$

Next, we will investigate the MBP-preservation of the second-order in time scheme (3.13) for the cases of $d = 2$ and $L_2 + L_3 = 0$ for $d = 3$, which can be written as follows: given the initial values of (Q_h^0, s^0) , we find $(Q_h^{n+1}, s^{n+1}) \in \mathbb{S}_h^d, \mathbb{R}, d = 2, 3, n \geq 1$ such

that

$$(3.28a) \quad \begin{aligned} & \left(\left(\frac{2}{\tau} + \kappa g(Q_{*,h}^{n+\frac{1}{2}}, s_*^{n+\frac{1}{2}}) \right) I - L\Delta_h \right) Q_h^{ij,n+1} \\ & = \left(\left(\frac{2}{\tau} - \kappa g(Q_{*,h}^{n+\frac{1}{2}}, s_*^{n+\frac{1}{2}}) \right) I + L\Delta_h \right) Q_h^{ij,n} \\ & \quad + 2g(Q_{*,h}^{n+\frac{1}{2}}, s_*^{n+\frac{1}{2}}) (\kappa Q_{*,h}^{ij,n+\frac{1}{2}} + f(Q_{*,h}^{ij,n+\frac{1}{2}})), \end{aligned}$$

$$(3.28b) \quad \begin{aligned} s^{n+1} = & s^n - g(Q_{*,h}^{n+\frac{1}{2}}, s_*^{n+\frac{1}{2}}) \sum_{i,j=1}^3 \langle f(Q_{*,h}^{ij,n+\frac{1}{2}}), Q_h^{ij,n+1} - Q_h^{ij,n} \rangle_h \\ & + \kappa g(Q_{*,h}^{n+\frac{1}{2}}, s_*^{n+\frac{1}{2}}) \sum_{i,j=1}^3 \langle Q_h^{ij,n+\frac{1}{2}} - Q_{*,h}^{ij,n+\frac{1}{2}}, Q_h^{ij,n+1} - Q_h^{ij,n} \rangle_h, \end{aligned}$$

where $[Q_{*,h}^{n+\frac{1}{2}}, s_*^{n+\frac{1}{2}}] = \text{MBP-sESAV1}(Q^n, s^n, \tau/2)$. For convenience, we will refer to the above scheme as the MBP-sESAV2 scheme hereafter. Then, the vector form of the MBP-sESAV2 scheme (3.28) reads

$$(3.29a) \quad \widehat{\mathbb{G}}_h \vec{Q}_h^{ij,n+1} = \overline{\mathbb{G}}_h \vec{Q}_h^{ij,n} + 2g(Q_{*,h}^{n+\frac{1}{2}}, s_*^{n+\frac{1}{2}}) (\kappa \vec{Q}_{*,h}^{ij,n+\frac{1}{2}} + f(\vec{Q}_{*,h}^{ij,n+\frac{1}{2}})),$$

$$(3.29b) \quad \begin{aligned} s^{n+1} = & s^n - g(Q_{*,h}^{n+\frac{1}{2}}, s_*^{n+\frac{1}{2}}) \sum_{i,j=1}^3 \langle f(\vec{Q}_{*,h}^{ij,n+\frac{1}{2}}), \vec{Q}_h^{ij,n+1} - \vec{Q}_h^{ij,n} \rangle_h \\ & + \kappa g(Q_{*,h}^{n+\frac{1}{2}}, s_*^{n+\frac{1}{2}}) \sum_{i,j=1}^3 \langle \vec{Q}_h^{ij,n+\frac{1}{2}} - \vec{Q}_{*,h}^{ij,n+\frac{1}{2}}, \vec{Q}_h^{ij,n+1} - \vec{Q}_h^{ij,n} \rangle_h. \end{aligned}$$

with matrices $\widehat{\mathbb{G}}_h$ and $\overline{\mathbb{G}}_h$ defined respectively by

$$(3.30) \quad \widehat{\mathbb{G}}_h := \left(\frac{2}{\tau} + \kappa g(Q_{*,h}^{n+\frac{1}{2}}, s_*^{n+\frac{1}{2}}) \right) I - LD_h, \quad \overline{\mathbb{G}}_h := \left(\frac{2}{\tau} - \kappa g(Q_{*,h}^{n+\frac{1}{2}}, s_*^{n+\frac{1}{2}}) \right) I + LD_h,$$

where $[\vec{Q}_{*,h}^{n+\frac{1}{2}}, s_*^{n+\frac{1}{2}}] = \text{MBP-sESAV1}(\vec{Q}^n, s^n, \tau/2)$.

Theorem 3.10 *For $\eta^{(d)}$ given in (2.3) and (2.4), if κ satisfies (3.25), and*

$$(3.31) \quad \tau \leq \left(\frac{\kappa G^*}{2} + \frac{2^{d-1}L}{h^2} \right)^{-1},$$

where $G^* > 0$ is defined in Corollary 3.9. Then the MBP-sESAV2 scheme (3.28) preserves the MBP for $\{\vec{Q}_h^n\}$, i.e., $\|\vec{Q}_h^n\|_{F,\infty} \leq \eta$, is valid for $n \geq 0$.

Proof. Suppose $\|\vec{Q}^k\|_{F,\infty} \leq \eta^{(d)}$ for $n \geq 0$, and $(\vec{Q}_{*,h}^{n+\frac{1}{2}}, s_*^{n+\frac{1}{2}})$ is given by the MBP-sESAV1 scheme (3.14). Then, we derive from Theorem 3.8 and Corollary 3.9 that $\|\vec{Q}_{*,h}^{n+\frac{1}{2}}\|_{F,\infty} \leq \eta^{(d)}$ and $g(\vec{Q}_{*,h}^{n+\frac{1}{2}}, s_*^{n+\frac{1}{2}}) \leq G^*$. From the definitions of D_h in (3.16) and \widehat{G}_h , it follows that

$$\widehat{G}_h^{-1} \geq 0, \quad \|\widehat{G}_h^{-1}\|_\infty \leq \left(\frac{2}{\tau} + \kappa g(Q_{*,h}^{n+\frac{1}{2}}, s_*^{n+\frac{1}{2}}) \right)^{-1}$$

where we have used Lemma 3.4. Moreover, under the condition (3.31) together with the definition of D_h , we derive that

$$\overline{\mathbb{G}}_h = \left(\frac{2}{\tau} - \kappa g(Q_{*,h}^{n+\frac{1}{2}}, s_*^{n+\frac{1}{2}}) \right) I + LD_h \geq 0,$$

which means all the elements of $\bar{\mathbb{G}}_h$ are non-negative. In addition, together with $\sum_{l=1}^{(M+1)^d} (D_h)_{kl} = 0$ for any $k = 1, 2, \dots, (M+1)^d$, we obtain

$$\|\bar{\mathbb{G}}_h\|_\infty = \frac{2}{\tau} - \kappa g(Q_{*,h}^{n+\frac{1}{2}}, s_*^{n+\frac{1}{2}}).$$

Furthermore, using (3.29a), Lemma 3.5 and Lemma 3.6 gives
(3.32)

$$\begin{aligned} |\vec{Q}_h^{ij,n+1}|_F &= \sqrt{\sum_{i,j}^d (\vec{Q}_h^{ij,n+1})^{*2}} \\ &= \sqrt{\sum_{i,j}^d \left[\widehat{\mathbb{G}}_h^{-1} \left(\bar{\mathbb{G}}_h \vec{Q}_h^{ij,n} + 2g(Q_{*,h}^{n+\frac{1}{2}}, s_*^{n+\frac{1}{2}}) (\kappa \vec{Q}_{*,h}^{ij,n+\frac{1}{2}} + f(\vec{Q}_{*,h}^{ij,n+\frac{1}{2}})) \right) \right]^{*2}} \\ &\leq \widehat{\mathbb{G}}_h^{-1} \left[\bar{\mathbb{G}}_h \sqrt{\sum_{i,j}^d (\vec{Q}_h^{ij,n})^{*2}} + 2g(Q_{*,h}^{n+\frac{1}{2}}, s_*^{n+\frac{1}{2}}) \sqrt{\sum_{i,j}^d (\kappa \vec{Q}_{*,h}^{ij,n+\frac{1}{2}} + f(\vec{Q}_{*,h}^{ij,n+\frac{1}{2}}))^{*2}} \right] \\ &\leq \widehat{\mathbb{G}}_h^{-1} \left[\bar{\mathbb{G}}_h |\vec{Q}_h^{ij,n}|_F + 2g(Q_{*,h}^{n+\frac{1}{2}}, s_*^{n+\frac{1}{2}}) (\kappa |\vec{Q}_{*,h}^{ij,n+\frac{1}{2}}|_F + \bar{f}(|\vec{Q}_{*,h}^{ij,n+\frac{1}{2}}|_F)) \right] \end{aligned}$$

Then, it follows from the above inequality, Lemma 3.4 and Lemma 3.7 that

$$\begin{aligned} (3.33) \quad & \|\vec{Q}_h^{ij,n+1}|_F\|_\infty \\ & \leq \left\| \widehat{\mathbb{G}}_h^{-1} \left[\bar{\mathbb{G}}_h |\vec{Q}_h^{ij,n}|_F + 2g(Q_{*,h}^{n+\frac{1}{2}}, s_*^{n+\frac{1}{2}}) (\kappa |\vec{Q}_{*,h}^{ij,n+\frac{1}{2}}|_F + \bar{f}(|\vec{Q}_{*,h}^{ij,n+\frac{1}{2}}|_F)) \right] \right\|_\infty \\ & \leq \|\widehat{\mathbb{G}}_h^{-1}\|_\infty \left[\|\bar{\mathbb{G}}_h\|_\infty \|\vec{Q}_h^{ij,n}|_F\|_\infty + 2g(Q_{*,h}^{n+\frac{1}{2}}, s_*^{n+\frac{1}{2}}) \|\kappa |\vec{Q}_{*,h}^{ij,n+\frac{1}{2}}|_F + \bar{f}(|\vec{Q}_{*,h}^{ij,n+\frac{1}{2}}|_F)\|_\infty \right] \\ & \leq \left(\frac{2}{\tau} + \kappa g(Q_{*,h}^{n+\frac{1}{2}}, s_*^{n+\frac{1}{2}}) \right)^{-1} \left[\left(\frac{2}{\tau} - \kappa g(Q_{*,h}^{n+\frac{1}{2}}, s_*^{n+\frac{1}{2}}) \right) \eta^{(d)} + 2g(Q_{*,h}^{n+\frac{1}{2}}, s_*^{n+\frac{1}{2}}) \kappa \eta^{(d)} \right] \\ & = \eta^{(d)}, \end{aligned}$$

which completes the proof. \square

We also derive that both $G_* \leq g(Q_h^n, s^n) \leq G^*$ and $G_* \leq g(Q_{*,h}^{n+\frac{1}{2}}, s_*^{n+\frac{1}{2}}) \leq G^*$, which is similar to the analysis for the MBP-sESAV1 scheme (3.14) in Corollary 3.9.

4. Error Estimates. In this section, we carry out rigorous error estimates for the fully discrete second-order MBP-sESAV scheme (3.28).

For simplicity, we define the error functions as follows:

$$\begin{aligned} e_Q^{ij,n} &= Q_h^{ij,n} - Q_e^{ij}(t_n), \quad e_s^n = s^n - s_e(t_n). \\ e_{*,Q}^{ij,n+\frac{1}{2}} &= Q_{*,h}^{ij,n+\frac{1}{2}} - Q_e^{ij}(t_{n+\frac{1}{2}}), \quad e_{*,s}^{n+\frac{1}{2}} = s_*^{n+\frac{1}{2}} - s_e(t_{n+\frac{1}{2}}), \end{aligned}$$

where $Q_e^{ij}(t)$ and $s_e(t)$ represent the corresponding exact solutions, respectively.

Firstly, we shall provide estimates for $e_{*,Q}^{n+\frac{1}{2}}$ and $e_{*,s}^{n+\frac{1}{2}}$, which will be used in the derivation of error estimate for the MBP-sESAV2 scheme (3.28).

Lemma 4.1 *Under the assumption of Theorem 3.8, we have*

$$(4.1) \quad \|e_{*,Q}^{n+\frac{1}{2}}\|_h + |e_{*,s}^{n+\frac{1}{2}}| \leq C(\|e_Q^n\|_h + |e_s^n| + \tau(\tau + h^2)),$$

where the constant C depends on C_* , $|\Omega|$, G^* , Q_e , and $\|f\|_{C^1\{Q:|Q|\leq\eta\}}$.

Proof. From (3.2) and (3.14), we deduce error equations with respect to $e_{*,Q}^{ij,n+\frac{1}{2}}$ and $e_{*,s}^{n+\frac{1}{2}}$ as follows:

$$(4.2a) \quad \left(\frac{2}{\tau} + \kappa g(Q_h^n, s^n) \right) (e_{*,Q}^{ij,n+\frac{1}{2}} - e_Q^{ij,n}) - L\Delta_h e_{*,Q}^{ij,n+\frac{1}{2}} = J_{1,h}^{ij,n} + J_{2,h}^{ij,n} - R_{1,Q}^{ij,n},$$

$$(4.2b) \quad \begin{aligned} \frac{e_{*,s}^{n+\frac{1}{2}} - e_s^n}{\tau/2} &= -g(Q_h^n, s^n) \sum_{i,j=1}^3 \left\langle f(Q_h^{ij,n}), \frac{e_{*,Q}^{n+\frac{1}{2}} - e_Q^{ij,n}}{\tau/2} \right\rangle_h \\ &\quad - \sum_{i,j=1}^3 \left\langle J_{1,h}^{ij,n}, \frac{Q_e^{ij}(t_{n+\frac{1}{2}}) - Q_e^{ij}(t_n)}{\tau/2} \right\rangle_h - R_{1,s}^n, \end{aligned}$$

where the grid tensor functions $J_{1,h}^n$ and $J_{2,h}^n$ for $1 \leq i, j \leq d$ are given by

$$\begin{aligned} J_{1,h}^{ij,n} &:= g(Q_h^n, s^n) f(Q_h^{ij,n}) - f(Q_e^{ij}(t_{n+\frac{1}{2}})), \\ J_{2,h}^{ij,n} &:= -\kappa g(Q_h^n, s^n) (Q_e^{ij}(t_{n+\frac{1}{2}}) - Q_e^{ij}(t_n)), \end{aligned}$$

and the corresponding truncation errors $R_{1,Q}^n$ and $R_{1,s}^n$ can be estimated as follows:

$$(4.3) \quad \|R_{1,Q}^n\|_h \leq C(\tau + h^2), \quad |R_{1,s}^n| \leq C(\tau + h^2).$$

Taking the discrete inner product of (4.2a) with $\tau e_{*,Q}^{ij,n+\frac{1}{2}}$, summing up i, j from 1 to d , and using Young's inequality, we can obtain that

$$(4.4) \quad \begin{aligned} &\left(1 + \frac{\kappa g(Q_h^n, s^n) \tau}{2} \right) (\|e_{*,Q}^{n+\frac{1}{2}}\|_h^2 - \|e_Q^n\|_h^2 + \|e_{*,Q}^{n+\frac{1}{2}} - e_Q^n\|_h^2) + L\tau \|\nabla_h e_{*,Q}^{n+\frac{1}{2}}\|_h^2 \\ &= \tau \sum_{i,j=1}^3 \left\langle J_{1,h}^{ij,n} + J_{2,h}^{ij,n} - R_{1,Q}^{ij,n}, e_{*,Q}^{ij,n+\frac{1}{2}} \right\rangle_h \\ &\leq \frac{\tau^2}{2} (\|J_{1,h}^n\|_h^2 + \|J_{2,h}^n\|_h^2 + \|R_{1,Q}^n\|_h^2) + \frac{1}{2} \|e_{*,Q}^{n+\frac{1}{2}}\|_h^2. \end{aligned}$$

Thus, together with (4.3) and Corollary 3.9, we deduce that

$$(4.5) \quad \|e_{*,Q}^{n+\frac{1}{2}}\|_h^2 \leq 2\|e_Q^n\|_h^2 + \tau^2 \|J_{1,h}^n\|_h^2 + C_{Q_e} \kappa G^* \tau^4 + C\tau^2(\tau + h^2)^2.$$

Noting that $\|Q_e(t_n)\|_\infty \leq \eta^{(d)}$, $\|\tilde{Q}_h^n(t_n)\|_{F,\infty} \leq \eta^{(d)}$ and the uniform bounds of s_e and s^n , we next give an estimation for the term $J_{1,h}^n$. Denote the term $g(Q_h^n, s^n) - g(Q_e(t_n), s_e(t_n))$ by $J_{3,h}^n$, then we have

$$(4.6) \quad \begin{aligned} |J_{3,h}^n| &\leq |g(Q_h^n, s^n) - g(Q_h^n, s_e(t_n))| + |g(Q_h^n, s_e(t_n)) - g(Q_e(t_n), s_e(t_n))| \\ &:= A_1 + A_2. \end{aligned}$$

In addition, we deduce that

$$\begin{aligned} A_1 &= \frac{1}{\exp\{\mathcal{E}_{1h}(Q_h^n)\}} |\exp(s^n) - \exp\{s_e(t_n)\}| \leq C_g |e_s^n|, \\ A_2 &= \exp\{s_e(t_n)\} \left| \frac{1}{\exp\{\mathcal{E}_{1h}(Q_h^n)\}} - \frac{1}{\exp\{\mathcal{E}_{1h}(Q_e(t_n))\}} \right| \\ &\leq \exp\{\mathcal{E}(Q_h^0) + C_*\} |\mathcal{E}_{1h}(Q_h^n) - \mathcal{E}_{1h}(Q_e(t_n))| \\ &\leq C_g \|e_Q^n\|_h, \end{aligned}$$

where the constant C_g depends on C_* , $|\Omega|$. Hence, $J_{3,h}^n$ can be bounded by

$$(4.7) \quad |J_{3,h}^n| \leq C_g(\|e_Q^n\|_h + |e_s^n|).$$

Furthermore, we use triangle inequality and Hölder's inequality to obtain

$$(4.8) \quad \begin{aligned} \|J_{1,h}^n\|_h &\leq \|g(Q_h^n, s^n)(f(Q_h^n) - f(Q_e(t_n)))\|_h + \|J_{3,h}^n f(Q_e(t_n))\|_h \\ &\quad + \|f(Q_e(t_n)) - f(Q_e(t_{n+\frac{1}{2}}))\|_h \\ &\leq \|f'\|_{C\{Q:|Q|_F \leq \eta^{(d)}\}} [G^* \|e_Q^n\|_h + C_{Q_e} \tau] + \|f(Q_e(t_n))\|_h |J_{3,h}^n| |\Omega| \\ &\leq C(\|e_Q^n\|_h + |e_s^n| + \tau), \end{aligned}$$

where the constant C depends on C_g , G^* and $\|f\|_{C^1\{Q:|Q| \leq \eta\}}$. Substituting (4.8) into (4.5), we get

$$(4.9) \quad \|e_{*,Q}^{n+\frac{1}{2}}\|_h^2 \leq C \left(\|e_Q^n\|_h^2 + \tau^2 |e_s^n|^2 + \tau^2 (\tau + h^2)^2 \right).$$

By multiplying (4.2b) by $\tau e_{*,s}^{n+\frac{1}{2}}$ and utilizing (4.3), (4.8), (4.9), and Young's inequality, we can obtain that

$$\begin{aligned} &(|e_{*,s}^{n+\frac{1}{2}}|^2 - |e_s^n|^2 + |e_{*,s}^{n+\frac{1}{2}} - e_s^n|^2) \\ &= -e_{*,s}^{n+\frac{1}{2}} \left[2g(Q_h^n, s^n) \sum_{i,j=1}^3 \left\langle f(Q_h^{ij,n}), e_{*,Q}^{ij,n+\frac{1}{2}} - e_Q^{ij,n} \right\rangle_h \right. \\ &\quad \left. + 2 \sum_{i,j=1}^3 \left\langle J_{1,h}^{ij,n}, Q_e^{ij}(t_{n+\frac{1}{2}}) - Q_e^{ij}(t_n) \right\rangle_h + \tau R_{1,s}^n \right] \\ &\leq \frac{1}{2} |e_{*,s}^{n+\frac{1}{2}}|^2 + C \left[\|e_{*,Q}^{ij,n+\frac{1}{2}}\|_h^2 + \|e_Q^{ij,n}\|_h^2 + \|J_{1,h}^n\|_h^2 \tau^2 + \tau^2 (\tau + h^2)^2 \right] \\ &\leq \frac{1}{2} |e_{*,s}^{n+\frac{1}{2}}|^2 + C \left[\|e_Q^n\|_h^2 + \tau^2 |e_s^n|^2 + \tau^2 (\tau + h^2)^2 \right]. \end{aligned}$$

Thus, we derive that

$$(4.10) \quad |e_{*,s}^{n+\frac{1}{2}}|^2 \leq 2 |e_s^n|^2 + C \left[\|e_Q^n\|_h^2 + \tau^2 |e_s^n|^2 + \tau^2 (\tau + h^2)^2 \right].$$

Combing (4.9) and (4.10) together, we obtain the desired results (4.1). \square

Theorem 4.2 (Error estimate of MBP-sESAV2) *Under the assumption of Theorem 3.10, it holds for the MBP-sESAV2 scheme (3.28) that*

$$(4.11) \quad \|e_Q^n\| + \|\nabla_h e_Q^n\| + |e_s^n| \leq C(\tau^2 + h^2), \quad 0 \leq n \leq \lfloor T/\tau \rfloor,$$

where the constant C depends on C_* , $|\Omega|$, G_* , G^* , Q_e , T , and $\|f\|_{C^1\{Q:|Q| \leq \eta\}}$.

Proof. It follows from (3.2) and (3.28) that the error equations with respect to $e_Q^{ij,n+1}$ and e_s^{n+1} read as

$$(4.12a) \quad \begin{aligned} &\frac{e_Q^{ij,n+1} - e_Q^{ij,n}}{\tau} - L\Delta_h \frac{e_Q^{ij,n+1} + e_Q^{ij,n}}{2} + \kappa g(Q_{*,h}^{n+\frac{1}{2}}, s_*^{n+\frac{1}{2}}) \frac{e_Q^{ij,n+1} + e_Q^{ij,n}}{2} \\ &= J_{1*,h}^{ij,n} + J_{2*,h}^{ij,n} + \kappa g(Q_{*,h}^{n+\frac{1}{2}}, s_*^{n+\frac{1}{2}}) e_{*,Q}^{ij,n+\frac{1}{2}} - R_{2,Q}^{ij,n}, \end{aligned}$$

$$\begin{aligned}
\frac{e_s^{n+1} - e_s^n}{\tau} &= -g(Q_{*,h}^{n+\frac{1}{2}}, s_*^{n+\frac{1}{2}}) \sum_{i,j=1}^3 \left\langle f(Q_{*,h}^{ij,n+\frac{1}{2}}), \frac{e_Q^{ij,n+1} - e_Q^{ij,n}}{\tau} \right\rangle_h \\
(4.12b) \quad &\quad - \sum_{i,j=1}^3 \left\langle J_{1*,h}^{ij,n}, \frac{Q_e^{ij}(t_{n+1}) - Q_e^{ij}(t_n)}{\tau} \right\rangle_h - R_{2,s}^n,
\end{aligned}$$

where the grid tensor functions $J_{1*,h}^n$ and $J_{2*,h}^n$ for $1 \leq i, j \leq d$ are given by

$$\begin{aligned}
J_{1*,h}^{ij,n} &:= g(Q_{*,h}^{n+\frac{1}{2}}, s_*^{n+\frac{1}{2}}) f(Q_{*,h}^{ij,n+\frac{1}{2}}) - f(Q_e^{ij}(t_{n+\frac{1}{2}})), \\
J_{2*,h}^{ij,n} &:= -\kappa g(Q_{*,h}^{n+\frac{1}{2}}, s_*^{n+\frac{1}{2}}) \left(\frac{Q_e^{ij}(t_{n+1}) + Q_e^{ij}(t_n)}{2} - Q_e^{ij}(t_{n+\frac{1}{2}}) \right),
\end{aligned}$$

and the truncation errors R_{2Q}^n and R_{2s}^n satisfy

$$\|R_{2Q}^n\| \leq C(\tau^2 + h^2), \quad |R_{2s}^n| \leq C(\tau^2 + h^2).$$

Taking the discrete inner product of (4.12a) with $e_Q^{ij,n+1} - e_Q^{ij,n}$ and summing up for $1 \leq i, j \leq 3$, we arrive at

$$\begin{aligned}
(4.13) \quad &\frac{1}{\tau} \|e_Q^{n+1} - e_Q^n\|_h^2 + \frac{1}{2} [\kappa G_*(\|e_Q^{n+1}\|_h^2 - \|e_Q^n\|_h^2) + L(\|\nabla_h e_Q^{n+1}\|_h^2 - \|\nabla_h e_Q^n\|_h^2)] \\
&= \sum_{i,j=1}^3 \left\langle J_{1*,h}^{ij,n} + J_{2*,h}^{ij,n} + \kappa g(Q_{*,h}^{n+\frac{1}{2}}, s_*^{n+\frac{1}{2}}) e_{*,Q}^{ij,n+\frac{1}{2}} - R_{2Q}^n, e_Q^{ij,n+1} - e_Q^{ij,n} \right\rangle_h \\
&\leq \frac{1}{2\tau} \|e_Q^{n+1} - e_Q^n\|_h^2 + C\tau (\|J_{1*,h}^n\|_h^2 + \|e_{*,Q}^{n+\frac{1}{2}}\|_h^2 + (\tau^2 + h^2)^2).
\end{aligned}$$

where we have used Young's inequality and $0 < G_* \leq g(Q_{*,h}^{n+\frac{1}{2}}, s_*^{n+\frac{1}{2}}) \leq G^*$. By following a similar process of deriving the estimate for $J_{1*,h}^n$ in Lemma 4.1, we can obtain a similar estimate for $J_{1*,h}^n$ as follows:

$$\|J_{1*,h}^n\|_h^2 \leq C(\|e_{*,Q}^{n+\frac{1}{2}}\|_h^2 + |e_{*,s}^{n+\frac{1}{2}}|^2).$$

Together with (4.13), we obtain

$$\begin{aligned}
(4.14) \quad &\frac{1}{2\tau} \|e_Q^{n+1} - e_Q^n\|_h^2 + \frac{1}{2} [\kappa G_*(\|e_Q^{n+1}\|_h^2 - \|e_Q^n\|_h^2) + L(\|\nabla_h e_Q^{n+1}\|_h^2 - \|\nabla_h e_Q^n\|_h^2)] \\
&\leq C\tau (\|e_{*,Q}^{n+\frac{1}{2}}\|_h^2 + |e_{*,s}^{n+\frac{1}{2}}|^2 + (\tau^2 + h^2)^2).
\end{aligned}$$

Multiplying (4.12b) by $2\tau e_s^{n+1}$ and using the Höder's inequality, yields

$$\begin{aligned}
(4.15) \quad &|e_s^{n+1}|^2 - |e_s^n|^2 + |e_s^{n+1} - e_s^n|^2 \\
&= -2e_s^{n+1} \left[g(Q_{*,h}^{n+\frac{1}{2}}, s_*^{n+\frac{1}{2}}) \sum_{i,j=1}^3 \left\langle f(Q_{*,h}^{ij,n+\frac{1}{2}}), e_Q^{ij,n+1} - e_Q^{ij,n} \right\rangle_h \right. \\
&\quad \left. - \sum_{i,j=1}^3 \left\langle J_{1*,h}^{ij,n}, Q_e^{ij}(t_{n+1}) - Q_e^{ij}(t_n) \right\rangle_h - \tau R_{2,s}^n \right] \\
&\leq C [|e_s^{n+1}| \|e_Q^{n+1} - e_Q^n\|_h + |e_s^{n+1}| \|J_{1*,h}^n\|_h \tau + \tau |e_s^{n+1}| |R_{2,s}^n|] \\
&\leq \frac{\|e_Q^{n+1} - e_Q^n\|_h^2}{2\tau} + C\tau [|e_s^{n+1}|^2 + \|e_{*,Q}^{n+\frac{1}{2}}\|_h^2 + |e_{*,s}^{n+\frac{1}{2}}|^2 + \tau^2(\tau + h^2)^2].
\end{aligned}$$

Summing up the inequalities (4.14) and (4.15), and using the Lemma 4.1, we derive

$$\begin{aligned}
 (4.16) \quad & \frac{1}{2} [\kappa G_*(\|e_Q^{n+1}\|_h^2 - \|e_Q^n\|_h^2) + L(\|\nabla_h e_Q^{n+1}\|_h^2 - \|\nabla_h e_Q^n\|_h^2)] + |e_s^{n+1}|^2 - |e_s^n|^2 \\
 & \leq C\tau(|e_s^{n+1}|^2 + \|e_{*,Q}^{n+\frac{1}{2}}\|_h^2 + |e_{*,s}^{n+\frac{1}{2}}|^2 + (\tau^2 + h^2)^2) \\
 & \leq C\tau(|e_s^{n+1}|^2 + \|e_Q^n\|_h^2 + |e_s^n|^2 + (\tau^2 + h^2)^2).
 \end{aligned}$$

Then (4.11) can be obtained by using the discrete Gronwall's inequality. \square

We shall only provide the main convergence results for the first-order MBP-sESAV scheme (3.14) below, as their proofs are essentially similar to those for the second-order scheme.

Theorem 4.3 (*Error estimate of sESAV1*) *For $\eta^{(d)}$ given in (2.3) and (2.4), assume that κ satisfies (3.25), then we have the error estimate for the MBP-sESAV1 scheme (3.14) as follows:*

$$\|e_Q^n\| + \|\nabla_h e_Q^n\| + |e_s^n| \leq C(\tau + h^2), \quad 0 \leq n \leq \lfloor T/\tau \rfloor,$$

where the constant C depends on $C_*, |\Omega|, G_*, G^*, Q_e, T$, and $\|f\|_{C^1\{Q:|Q|\leq\eta\}}$.

5. Numerical Simulations. In this section, we present various numerical experiments in 2D and 3D cases to verify the theoretical results derived in the previous section and demonstrate the supremum norms, the energy stability and the accuracy of the proposed numerical schemes. Moreover, the first-order scheme (3.8) and the second-order scheme (3.13) can be implemented by fast Discrete Sine Transform (DST) efficiently. For more information, see, e.g., [18]. Unless otherwise specified, we choose the second-order scheme (3.13) in the following simulation.

5.1. Convergence tests. In this subsection, we verify the accuracy of the proposed MBP-sESAV1 and MBP-sESAV2 schemes. In the following simulations, the constant κ is determined by $\kappa = 2$.

In this test, we take the model parameter values as

$$L_x = L_y = 1, \quad L = 1.0 \times 10^{-3}, \quad a = -0.25, \quad b = 1, \quad c = 1.$$

For the initial condition, we take

$$Q_0 = \mathbf{n}_0 \mathbf{n}_0^T - \frac{\|\mathbf{n}_0\|_h^2}{2} \mathbf{I}, \quad \mathbf{n}_0 = (\sin(2\pi x) \sin(2\pi y), \sin(2\pi x) \sin(2\pi y))^T.$$

5.1.1. Refinement in space. We first test convergence rates of space for the second-order scheme (3.13). Particularly, $\|e_\xi\| = \|\xi_h - \xi_{h/2}\|$ determines the errors between the two distinct grid spacings h and $h/2$. The reference solution is computed with 2×10^4 time steps. The errors at $T = 1$, measured in the L^2 norm with different time steps are shown in Table 1, where we can get the second-order convergence in the space direction clearly.

5.1.2. Refinement in time. Next, we give convergence rates of time for the first-order scheme (3.8) and the second-order scheme (3.13). The reference solution is computed with 256 grid points in each spatial direction. The numerical results are listed in Tables 2 and 3 for the two MBP-sESAV schemes, which give solid supporting evidence for the expected first-order and second-order convergence in time.

TABLE 1
Error and convergence rates of second-order sESAV scheme (3.13).

h	$\ \nabla e_Q^n\ _{L^\infty(L^2)}$	Rate	$\ e_Q^n\ _{L^\infty(L^2)}$	Rate	$ e_s^n _{L^\infty(0,T)}$	Rate
1/32	1.46E-1	—	6.10E-3	—	4.71E-5	—
1/64	3.59E-2	2.03	1.40E-3	2.12	1.34E-5	1.81
1/128	9.00E-3	2.00	3.49E-4	2.02	3.29E-6	2.03
1/256	2.30E-3	2.00	8.70E-5	2.00	8.19E-7	2.01
1/512	5.64E-4	2.00	2.17E-5	2.00	2.05E-7	2.00

TABLE 2
Error and convergence rates of first-order sESAV scheme (3.8).

τ	$\ \nabla e_Q^n\ _{L^\infty(L^2)}$	Rate	$\ e_Q^n\ _{L^\infty(L^2)}$	Rate	$ e_s^n _{L^\infty(0,T)}$	Rate
1/32	2.51E-2	—	1.40E-3	—	1.10E-3	—
1/64	1.30E-2	0.95	7.16E-4	0.94	5.41E-4	1.00
1/128	6.60E-3	0.97	3.65E-4	0.97	2.71E-4	1.00
1/256	3.30E-3	0.99	1.85E-4	0.99	1.35E-4	1.00
1/512	1.70E-3	0.99	9.27E-5	0.99	6.76E-5	1.00

TABLE 3
Error and convergence rates of second-order sESAV scheme (3.13).

τ	$\ \nabla e_Q^n\ _{L^\infty(L^2)}$	Rate	$\ e_Q^n\ _{L^\infty(L^2)}$	Rate	$ e_s^n _{L^\infty(0,T)}$	Rate
1/32	4.52E-4	—	2.47E-5	—	3.71E-5	—
1/64	1.18E-4	1.94	6.43E-6	1.94	9.23E-6	2.01
1/128	3.00E-5	1.97	1.64E-6	1.97	2.29E-6	2.01
1/256	7.58E-6	1.99	4.14E-7	1.99	5.72E-7	2.00
1/512	1.90E-6	1.99	1.04E-7	1.99	1.43E-7	2.00

5.2. Disappearing hole. We use the value of the parameters:

$$L_x = L_y = 1, \quad L = 2.5 \times 10^{-3}, \quad a = -0.2, \quad c = 1, \quad \kappa = 2.$$

The initial data are given by

$$Q_0 = \frac{\mathbf{n}_0 \mathbf{n}_0^T}{\|\mathbf{n}_0\|_h^2} - \frac{1}{2} \mathbf{I}, \quad \mathbf{n}_0 = (x(1-x)y(1-y), \sin(2\pi x) \sin(2\pi y))^T.$$

In the computations, we choose space step $h_x = h_y = 1/50$ and time step $\tau = 1 \times 10^{-2}$. Figure 1 presents the major director orientation of the liquid crystal in the xy plane. It can be observed that the initial misalignment vanishes along the axes and then propagates in a shrinking circle toward the center of the domain and disappears eventually. Figure 2 shows that the difference between the two eigenvalues on the xy plane is a true measure of the orientation of liquid crystals. When the difference value is zero, it is called a defect. It represents a state of liquid crystal, indicating that the orientation on the xy plane is isotropic and dominant. The evolutions of the supremum norms and the energies of simulated solutions are shown in Figure 2 with different time steps. Our scheme preserves the MBP and the energy dissipation perfectly even with coarse time steps.

5.3. Dynamics of orientation in the liquid crystal. In this subsection, three examples are performed to show orientation dynamics in flows of liquid crystals numerically using the implemented linear scheme.

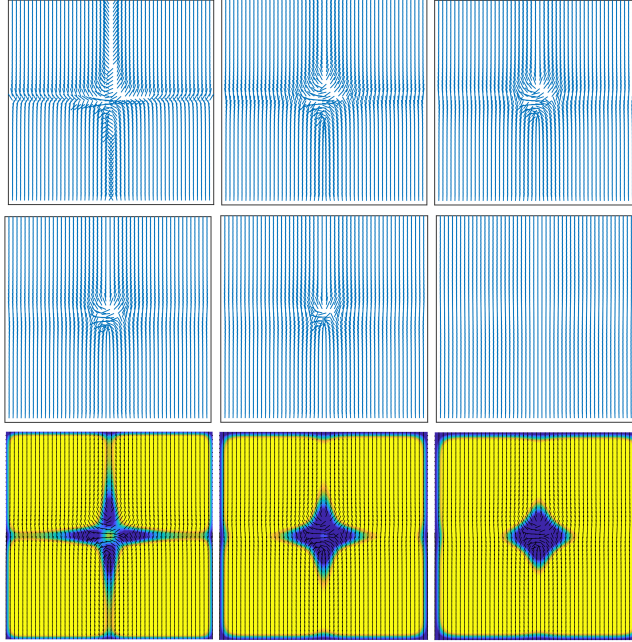


FIG. 1. Evolutions of disappearing holes at different time t . Snapshots are the major director orientation of the liquid crystal in the xy plane taken at $t = 0, 0.2, 0.4, 0.6, 0.8, 2.0$, respectively (top two rows). The difference of eigenvalues on the xy plane for $Q + \frac{1}{2}I$ at time $t = 0.2, 0.4, 0.6$, respectively (bottom row).

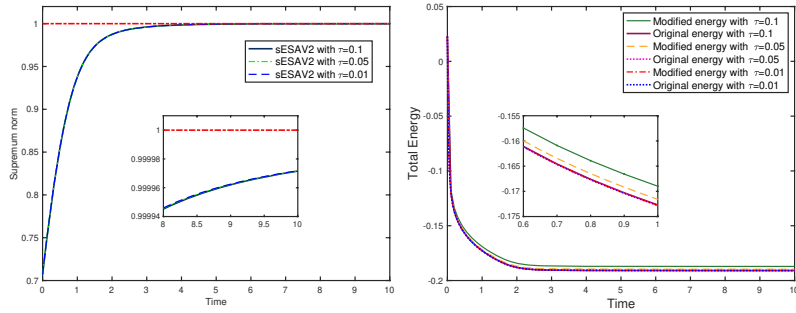


FIG. 2. Evolutions of the supremum norms (left) and the energies (right) of simulated solutions computed by MBP-sESAV2 (3.28) with $\tau = 0.1$, $\tau = 0.05$ and $\tau = 0.01$ respectively.

Example 1. We set the parameters as follows:

$$L_x = L_y = 2, \quad L = 1.0 \times 10^{-3}, \quad a = -4, \quad c = 4, \quad \kappa = 4.$$

The initial state for Q_0 is defined as

$$(5.1) \quad Q_0 = \frac{\mathbf{n}_0 \mathbf{n}_0^T}{\|\mathbf{n}_0\|_h^2} - \frac{1}{2} \mathbf{I}, \quad \mathbf{n}_0 = \begin{cases} (1, 0)^T, & x \in [0.5, 1.5] \times [0.5, 1.5]; \\ (0, 1)^T, & \text{otherwise.} \end{cases}$$

being the unit vector representing the direction of the liquid crystal at position x .

In this example, we choose $h_x = h_y = 1/50$ in the computations. Here, we adopt

the variable time step sizes τ_{n+1} updated by using the approach from [23]

$$\tau_{n+1} = \max\{\tau_{\min}, \frac{\tau_{\max}}{\sqrt{1 + \alpha|d_t \mathcal{E}_h[Q_h^n]|^2}}\},$$

where $d_t \mathcal{E}_h[Q_h^n] = (\mathcal{E}_h[Q_h^n] - \mathcal{E}_h[Q_h^n])/\tau_n$ and $\alpha > 0$ is a constant parameter. We choose the minimal and maximal time step sizes as $\tau_{\min} = 0.01$ and $\tau_{\max} = 0.2$, respectively, and set $\alpha = 10^5$.

Example 2. We choose the same parameters as Example 1 but other parameters are given as: $L_x = L_y = 4$, $L = 1.4 \times 10^{-2}$, $a = -6$, $c = 6$, $\kappa = 6$, with initial state

$$(5.2) \quad Q_0 = \frac{\mathbf{n}_0 \mathbf{n}_0^T}{\|\mathbf{n}_0\|_h^2} - \frac{1}{2} \mathbf{I}, \quad \mathbf{n}_0 = \begin{cases} (1, 0)^T, & x \in [0.25, 3.75] \times [0.25, 3.75]; \\ (0, 1)^T, & \text{otherwise}, \end{cases}$$

For the variable time step sizes τ_{n+1} , we choose the minimal and maximal time step sizes as $\tau_{\min} = 0.01$ and $\tau_{\max} = 0.085$, respectively, and set $\alpha = 10^5$.

Example 3. In this example, we simulate the orientation dynamics in 3D liquid crystal flow. For the parameters' values, we set

$$L_x = L_y = 2, \quad L = 1.0 \times 10^{-3}, \quad a = -1.25, \quad b = 0.25, \quad c = 1, \quad \kappa = 6.$$

The initial state for Q_0 is defined as $Q_0 = \mathbf{n}_0 \mathbf{n}_0^T / \|\mathbf{n}_0\|_h^2 - \frac{1}{3} \mathbf{I}$ with

$$\mathbf{n}_0 = \begin{cases} (1, 0, 0)^T, & x \in [1.15, 1.65] \times [0.75, 1.25] \times [0.35, 0.85]; \\ (0, 0, 1)^T, & x \in [0.35, 0.85] \times [0.75, 1.25] \times [1.15, 1.65]; \\ (0, 1, 0)^T, & \text{otherwise}. \end{cases}$$

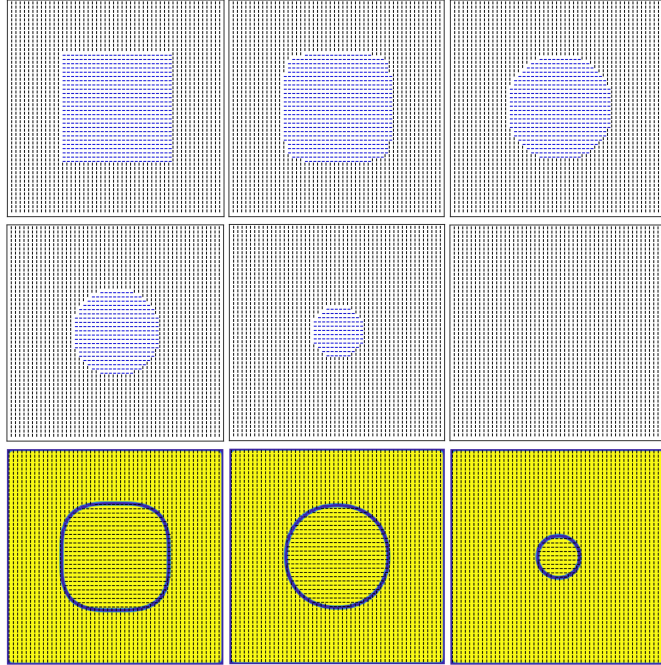


FIG. 3. (Example 1) Orientation of liquid crystal at different time t . Snapshots are the major director orientation of the liquid crystal in the xy plane taken at $t = 0, 20, 50, 100, 160, 200$, respectively (top two rows). The difference of eigenvalues on the xy plane for $Q + \frac{1}{2} I$ at time $t = 20, 50, 160$, respectively (bottom row).

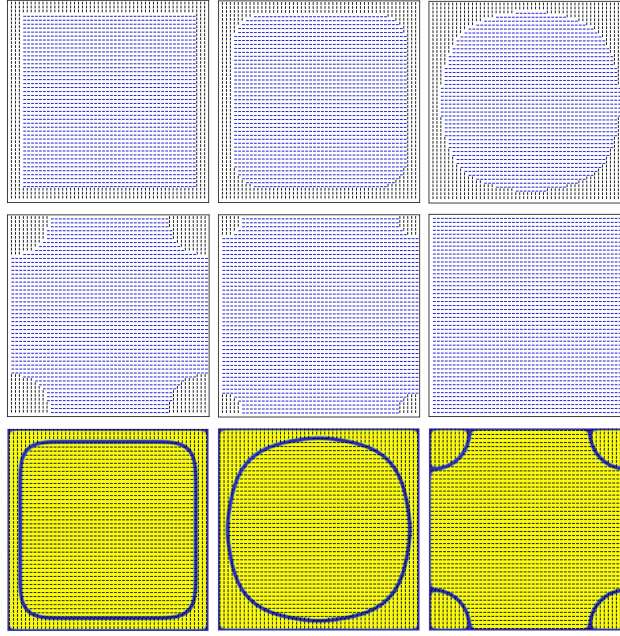
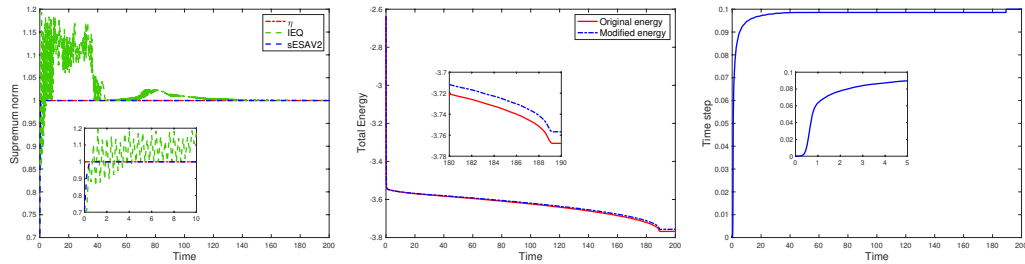
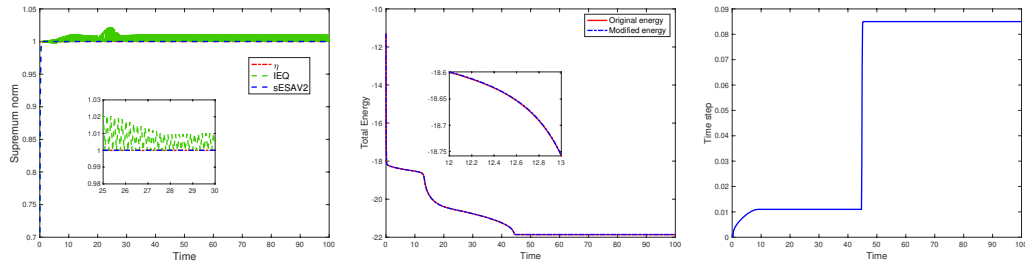


FIG. 4. (Example 2) Orientation of liquid crystal at different time t . Snapshots are the major director orientation of the liquid crystal in the xy plane taken at $t = 0, 3, 20, 45, 65, 100$, respectively (top two rows). The difference of eigenvalues on the xy plane for $Q + \frac{1}{2}I$ at time $t = 3, 20, 50$, respectively (bottom row).



Example 1 with final time $T = 200$.



Example 2 with final time $T = 100$.

FIG. 5. Evolutions in time of the supremum norms (left), the energies (middle) and the adaptive time steps (right).

The simulation is taken with $\tau = 1 \times 10^{-2}$ and $h_x = h_y = h_z = 1/50$ to discretize

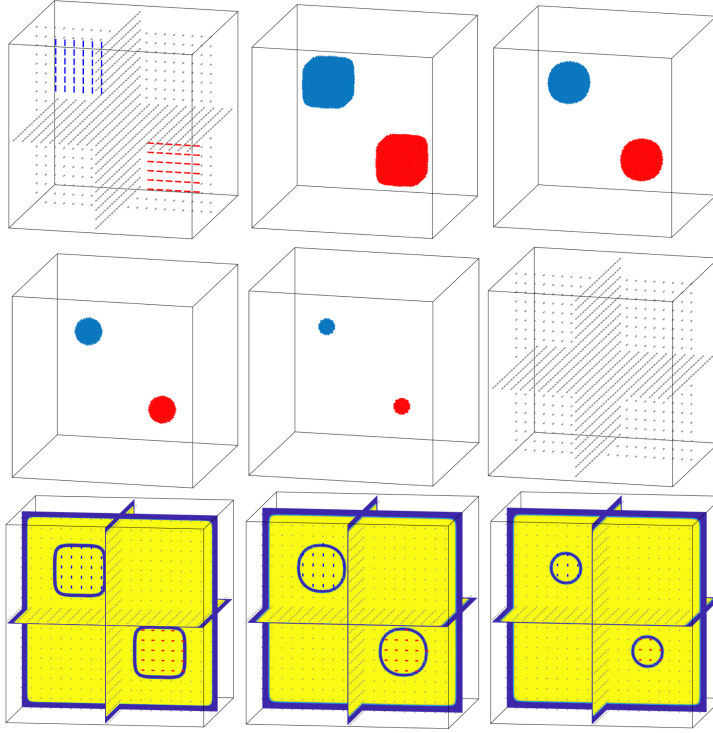


FIG. 6. (Example 3) Orientation of liquid crystal at different time t . Snapshots are the major director orientation of the liquid crystal in the xy plane taken at $t = 0, 2, 10, 18, 21, 30$, respectively (top two rows). The difference of eigenvalues on the xyz plane for $Q + \frac{1}{3}I$ at time $t = 2, 10, 18$, respectively (bottom row).

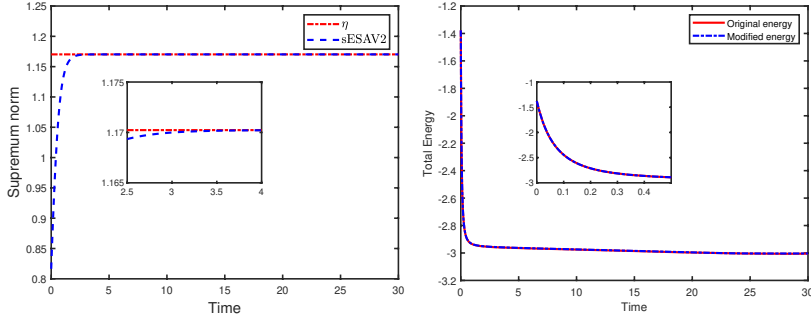


FIG. 7. (Example 3) Evolutions of the supremum norms (left) and the energies (right) of simulated solutions.

the time and space variables, respectively. The orientation of liquid crystal on the xy plane, which is denoted by \mathbf{n} , is mainly described by the dominant eigenvalue of Q . For the 2D case, the orientation of the liquid crystal is depicted in Figures 3 and 4. It can be observed that the final steady states are based on the initial values. Apparently, there are more vertical molecules than horizontal molecules at $T = 0$ in Figure 3. The set with horizontal molecules gets smaller with time, then the defects stay in a ring form and the ring shrinks with time. The liquid crystal directions

get closer to achieving a uniform vertical shape finally, i.e., the ring disappears. In contrast, there are more horizontal molecules than vertical molecules in Figure 4. The liquid crystal directions gradually reach the uniform horizontal configuration as the set of horizontal molecules expands toward the boundary.

The evolutions of the supremum norm of $|Q|$ and the energy of simulated solutions are displayed in Figure 5.3. The adaptive time-stepping approach increases computational efficiency significantly, especially for long-time simulations. The Comparison of the supremum norms of the simulated solutions based on the IEQ scheme and the MBP-sESAV2 approach with $\tau = 0.2$ and $\tau = 0.085$ are presented in the left of Figure 5.3. Figure 5.3 shows that our second-order scheme (3.13) performs better than the IEQ method presented in [8] with the same time step. Similar to the disappearing hole case, the sESAV schemes preserve the MBP and the energy dissipation law as expected. Similar results can be obtained for the 3D case in Figures 6-7. Moreover, it can also be verified that the maximum bound of the numerical scheme we obtained is bounded by the theoretical bound η .

6. Concluding remarks. In this paper, we proposed two linear and efficient schemes for the Q -tensor flow of liquid crystals based on the sESAV approach. The constructed schemes are unconditionally energy-stable and preserve the MBP. Moreover, we establish rigorous error estimates for the second-order scheme. One of the future research directions is to extend the approaches in this paper to hydrodynamic Q -tensor models, which couples a Navier-Stokes system for the fluid velocity with a parabolic reaction-convection-diffusion system.

REFERENCES

- [1] S. BADIA, F. GUILLÉN-GONZÁLEZ, AND J. V. GUTIÉRREZ-SANTACREU, *Finite element approximation of nematic liquid crystal flows using a saddle-point structure*, J. Comput. Phys., 230 (2011), pp. 1686–1706.
- [2] J. M. BALL AND A. ZARNESCU, *Orientability and energy minimization in liquid crystal models*, Arch. Ration. Mech. Anal., 202 (2011), pp. 493–535.
- [3] Y. CAI, J. SHEN, AND X. XU, *A stable scheme and its convergence analysis for a 2D dynamic Q -tensor model of nematic liquid crystals*, Math. Models Methods Appl. Sci., 27 (2017), pp. 1459–1488.
- [4] L. CHERFILS, A. MIRANVILLE, S. PENG, AND C. XU, *Analysis of discretized parabolic problems modeling electrostatic micro-electromechanical systems.*, Discrete Contin. Dyn. Syst. Ser. S, 12 (2019).
- [5] A. CONTRERAS, X. XU, AND W. ZHANG, *An elementary proof of eigenvalue preservation for the co-rotational Beris-Edwards system*, J. Nonlinear Sci., 29 (2019), pp. 789–801.
- [6] P. A. CRUZ, M. F. TOMÉ, I. W. STEWART, AND S. MCKEE, *Numerical solution of the ericksen-leslie dynamic equations for two-dimensional nematic liquid crystal flows*, J. Comput. Phys., 247 (2013), pp. 109–136.
- [7] P.-G. DE GENNES AND J. PROST, *The physics of liquid crystals*, no. 83, Oxford university press, 1993.
- [8] V. M. GUDIBANDA, F. WEBER, AND Y. YUE, *Convergence analysis of a fully discrete energy-stable numerical scheme for the Q -tensor flow of liquid crystals*, SIAM J. Numer. Anal., 60 (2022), pp. 2150–2181.
- [9] J. HAN, Y. LUO, W. WANG, P. ZHANG, AND Z. ZHANG, *From microscopic theory to macroscopic theory: a systematic study on modeling for liquid crystals*, Arch. Ration. Mech. Anal., 215 (2015), pp. 741–809.
- [10] Y. HAN, Y. HU, P. ZHANG, AND L. ZHANG, *Transition pathways between defect patterns in confined nematic liquid crystals*, J. Comput. Phys., 396 (2019), pp. 1–11.
- [11] D. HOU, H. WANG, AND C. ZHANG, *Positivity-preserving and unconditionally energy stable numerical schemes for mems model*, Appl. Numer. Math., 181 (2022), pp. 503–517.
- [12] Z. HU, S. M. WISE, C. WANG, AND J. S. LOWENGREB, *Stable and efficient finite-difference nonlinear-multigrid schemes for the phase field crystal equation*, J. Comput. Phys., 228

(2009), pp. 5323–5339.

[13] T. HUANG, F. LIN, C. LIU, AND C. WANG, *Finite time singularity of the nematic liquid crystal flow in dimension three*, Arch. Ration. Mech. Anal., 221 (2016), pp. 1223–1254.

[14] G. IYER, X. XU, AND A. D. ZARNESCU, *Dynamic cubic instability in a 2D q -tensor model for liquid crystals*, Mathematical Models and Methods in Applied Sciences, 25 (2015), pp. 1477–1517.

[15] K. JIANG, J. TONG, P. ZHANG, AND A.-C. SHI, *Stability of two-dimensional soft quasicrystals in systems with two length scales*, Phys. Rev. E, 92 (2015), p. 042159.

[16] L. JU, X. LI, AND Z. QIAO, *Generalized SAV-exponential integrator schemes for Allen-Cahn type gradient flows*, SIAM J. Numer. Anal., 60 (2022), pp. 1905–1931.

[17] L. JU, X. LI, AND Z. QIAO, *Stabilized exponential-SAV schemes preserving energy dissipation law and maximum bound principle for the Allen-Cahn type equations*, J. Sci. Comput., 92 (2022), pp. 1–34.

[18] L. JU, J. ZHANG, L. ZHU, AND Q. DU, *Fast explicit integration factor methods for semilinear parabolic equations*, J. Sci. Comput., 62 (2015), pp. 431–455.

[19] F.-H. LIN AND C. LIU, *Nonparabolic dissipative systems modeling the flow of liquid crystals*, Commun. Pure Appl. Math., 48 (1995), pp. 501–537.

[20] C. LIU, J. SHEN, AND X. YANG, *Dynamics of defect motion in nematic liquid crystal flow: modeling and numerical simulation*, Commun. Comput. Phys., 2 (2007), pp. 1184–1198.

[21] A. MAJUMDAR, *Equilibrium order parameters of nematic liquid crystals in the Landau-de Gennes theory*, Eur. J. Appl. Math., 21 (2010), pp. 181–203.

[22] H. MORI, E. C. GARTLAND JR, J. R. KELLY, AND P. J. BOS, *Multidimensional director modeling using the Q -tensor representation in a liquid crystal cell and its application to the π cell with patterned electrodes*, Japan. J. Appl. Phys., 38 (1999), p. 135.

[23] Z. QIAO, Z. ZHANG, AND T. TANG, *An adaptive time-stepping strategy for the molecular beam epitaxy models*, SIAM J. Sci. Comput., 33 (2011), pp. 1395–1414.

[24] J. SHEN, T. TANG, AND J. YANG, *On the maximum principle preserving schemes for the generalized Allen-Cahn equation*, Commun. Math. Sci., 14 (2016), pp. 1517–1534.

[25] J. SHEN, J. XU, AND J. YANG, *A new class of efficient and robust energy stable schemes for gradient flows*, SIAM Rev., 61 (2019), pp. 474–506.

[26] A. M. SONNET AND E. G. VIRGA, *Dissipative ordered fluids: theories for liquid crystals*, Springer Science & Business Media, 2012.

[27] O. M. TOVKACH, C. CONKLIN, M. C. CALDERER, D. GOLOVATY, O. D. LAVRENTOVICH, J. VINALS, AND N. J. WALKINGTON, *Q -tensor model for electrokinetics in nematic liquid crystals*, Phys. Rev. Fluid, 2 (2017), p. 053302.

[28] M. WANG, W. WANG, AND Z. ZHANG, *From the Q -tensor flow for the liquid crystal to the harmonic map flow*, Arch. Ration. Mech. Anal., 225 (2017), pp. 663–683.

[29] W. WANG, L. ZHANG, AND P. ZHANG, *Modelling and computation of liquid crystals*, Acta Numer., 30 (2021), pp. 765–851.

[30] Y. WANG AND J. XU, *Q -Tensor Gradient Flow with Quasi-Entropy and Discretizations Preserving Physical Constraints*, J. Sci. Comput., 94 (2023), pp. 1–29.

[31] H. WU, X. XU, AND A. ZARNESCU, *Dynamics and flow effects in the Beris-Edwards system modeling nematic liquid crystals*, Arch. Ration. Mech. Anal., 231 (2019), pp. 1217–1267.

[32] X. YANG, M. G. FOREST, H. LI, C. LIU, J. SHEN, Q. WANG, AND F. CHEN, *Modeling and simulations of drop pinch-off from liquid crystal filaments and the leaky liquid crystal faucet immersed in viscous fluids*, J. Comput. Phys., 236 (2013), pp. 1–14.

[33] J. ZHAO, X. YANG, Y. GONG, AND Q. WANG, *A novel linear second order unconditionally energy stable scheme for a hydrodynamic Q -tensor model of liquid crystals*, Comput. Methods Appl. Mech. Eng., 318 (2017), pp. 803–825.

[34] J. ZHAO, X. YANG, J. SHEN, AND Q. WANG, *A decoupled energy stable scheme for a hydrodynamic phase-field model of mixtures of nematic liquid crystals and viscous fluids*, J. Comput. Phys., 305 (2016), pp. 539–556.